CERES Terra & Aqua Edition4A SSF Cloud Properties - Accuracy and Validation

This section discusses the spectral radiances and cloud products included in the **SSF** data set version **Terra and Aqua MODIS Edition 4A**, hereafter denoted as Ed4. Additional information is in the Description/Abstract Guide. Cloud products in the SSF are the result of convolving the values for the clear-sky and cloudy data derived for each 1-km MODIS pixel sampled every fourth pixel and every other scan line (see Convolution Process) to give an effective resolution of 4 km to reduce processing time and data storage. Six primary radiances taken at 0.65 (visible, VIS), 1.24 (near infrared 1, NIR1), 2.13 (near infrared 2, NIR2), 3.79 (shortwave infrared, SIR), 11.0 (infrared, IR), and 12.0 (split-window channel, SWC) µm, channels 1, 5, 7, 20, 31, and 32, respectively, are used for each MODIS pixel. MODIS 0.469, 0.55, 0.858, 1.38, 6.72, 8.55 and 13.34-µm channels are also used for cloud detection in this version.

Terra and Aqua MODIS Radiance Calibrations

The cloud products rely on accurately calibrated imager radiances. Collection-5 (C5) MODIS validated radiance data were used, with some changes, for the Ed4 analyses. The MODIS thermal infrared channels are calibrated with onboard blackbodies and the solar channels are calibrated approximately once per month using a solar-viewing diffuser. Space looks provide zero radiance levels for the calibrations (Butler and Barnes, 1998). The Aqua channels were found to be very stable (Minnis et al. 2008a; Xiong et al. 2009; Wu et al. 2013) and therefore are not altered and serve as the references for adjusting the Terra calibrations. The Aqua 1.6-µm channel has previously been determined too noisy and unreliable with many missing pixels. Therefore, for consistency, no 1.6-µm data are used for either satellite. The 1.24 and 2.13-µm channels are used for cloud detection and secondary cloud particle size retrievals during processing of both the Aqua and Terra data. Differences between the Aqua and Terra MODIS calibrations in the VIS, NIR1, NIR2, and SIR channels were found through direct comparisons of matched Aqua and Terra data as in Minnis et al. (2008a). The following remarks summarize the calibration changes applied to the Terra MODIS data for the CERES Edition4A processing. The changes are based on matches of Aqua and Terra MODIS data from July 2002 – December 2011. Except for the Terra SIR channel, no calibration adjustments were applied for the period July 2002 to May 13, 2002. The calibration changes were evaluated by comparing matched Terra and Aqua data taken during 3 days of each month during 2003, 2008, and 2013. The MODIS Collection-6 (C6) data have been recently been released and include calibration upgrades to both Terra and Aqua. The Aqua changes appear to be negligible, while the magnitudes of the changes to Terra are variable.

The reflectances provided in the Terra MODIS C5 dataset were altered for three different periods beginning with the start of the Aqua period by multiplying the input reflectance by the correction factor, f_g:

$$f_g = a_0 + a_1 * DSL, \quad (1)$$

where DSL is the number of days since the launch of Aqua, 4 May 2002. No changes were applied prior to 14 May 2002. The calibration coefficients a_0 and a_1 are listed in Table 1.

Table 1. Calibration coefficients for Terra MODIS Collection 5 Ed4 reflectances/radiances.

Channel	14 May 2002 -18 Nov 2003		19 Nov 2003 – 31 March 2009		After 31 March 2009	
	a_0	a_1	a_0	a_1	a_0	a_1
1 (0.65 µm)	1.0100	0.0	1.0190	0.0	1.0320	0.0
2(0.87 µm)	0.9996	0.0	1.0010	2.904×10^{-6}	1.0059	0.0
3 (0.47 µm)	0.9958	1.182×10^{-5}	0.9997	9.662×10^{-6}	1.0368	0.0
4 (0.55 µm)	1.0016	0.0	1.0105	0.0	1.0219	0.0
5 (1.24 µm)	0.9724	0.0	0.9736	0.0	0.9706	0.0
7 (2.13 µm)	0.9927	0.0	0.9957	0.0	0.9995	0.0
26 (1.38 µm)	1.0307	0.0	1.0429	0.0	1.0430	0.0

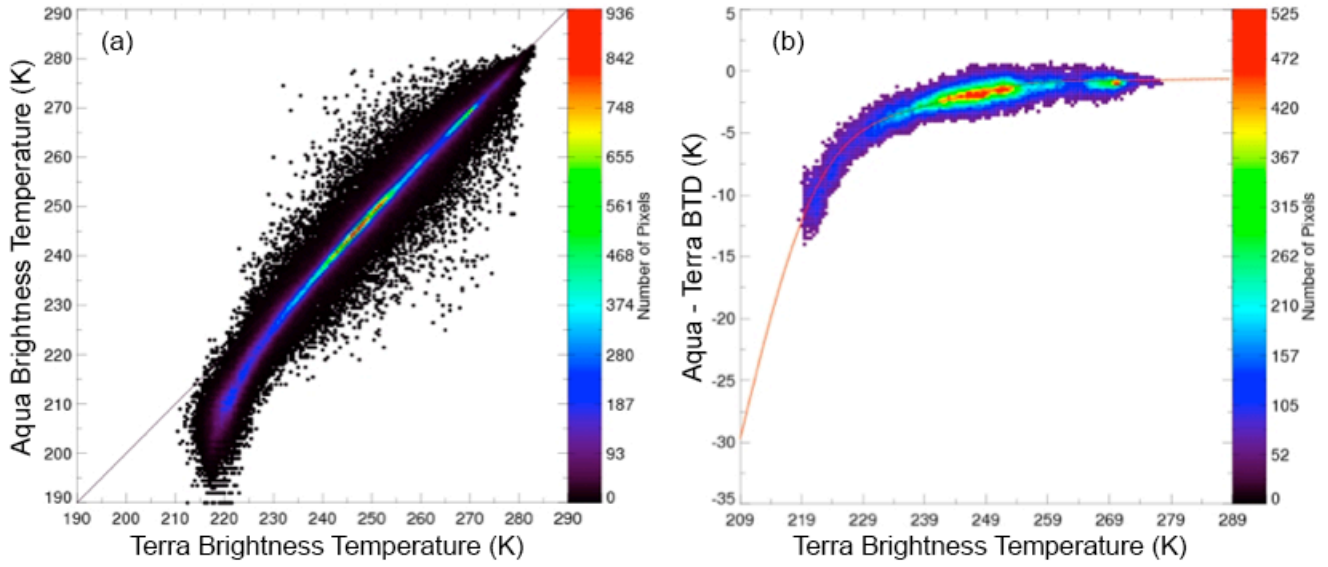

Figure 1. Scatterplots of (a) Aqua and Terra SIR temperatures for July 2007, and (b) the corresponding SIR temperature difference between Aqua and Terra as a function of Terra SIR temperatures. Red line is Terra 3.7 µm night time calibration curve for July 2007.

Ch 20, SIR (3.78 µm): Comparisons with Aqua MODIS between July 2002 and July 2005 show that the Terra MODIS measures SIR temperatures T_{Te} almost 0.55 K greater than Aqua during the daytime (Minnis et al. 2008b). Thus, 0.55 K is added during the daytime. During the night, T_{Te} can be from 1 – 3 K warmer than that from Aqua T_{Aq} when T_{Te} ~ 270 K up to 15 K warmer at T_{Te} ~ 220. The example in Figure 1 shows a scatterplot of Aqua and Terra SIR temperatures for July 2007 (Figure 1a) and the corresponding temperature differences between Aqua and Terra, T_{aq} - T_{Te}, as a function of T_{Te}. Such large differences between Aqua and Terra, especially at the low end, are seen in all MODIS C5 data records during nighttime. Seasonal Terra SIR calibration curves (red line in Figure 1b) were developed for each year by fitting values of T_{aq} - T_{Te} to a Gaussian error function as a function T_{Te}. Values are determined for a given month by linear interpolation in month from the center of the seasonal months: January, April, July, October. The curves are then used to correct the nominal Terra C5 temperatures at night during processing for the entire Terra record beginning in January 2000.

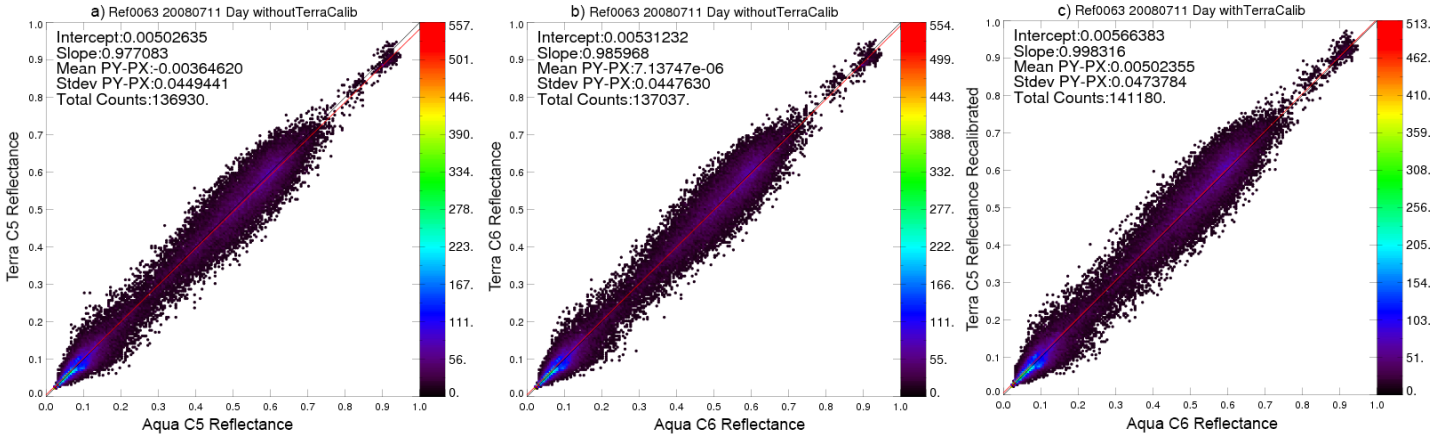

Figure 2. Visible (0.65 µm) reflectance comparisons between matched Terra and Aqua data, 11 July 2008. Colors indicate number of pixels for each reflectance pair. (a) C5 data, (b) C6 data, and (c) Aqua C6 and Terra C5 recalibrated using approach described in text.

Ch 31, IR (10.8 µm) and Ch 32, SWC (12.0 µm): Wan et al. (2002) found that the Terra MODIS infrared (IR) and split window (SWC) channels were accurate to ~0.4% or to ~± 0.2 K. Terra and Aqua temperatures for these channels show no differences during both daytime and nighttime. No calibration changes were made to Terra for either of these channels.

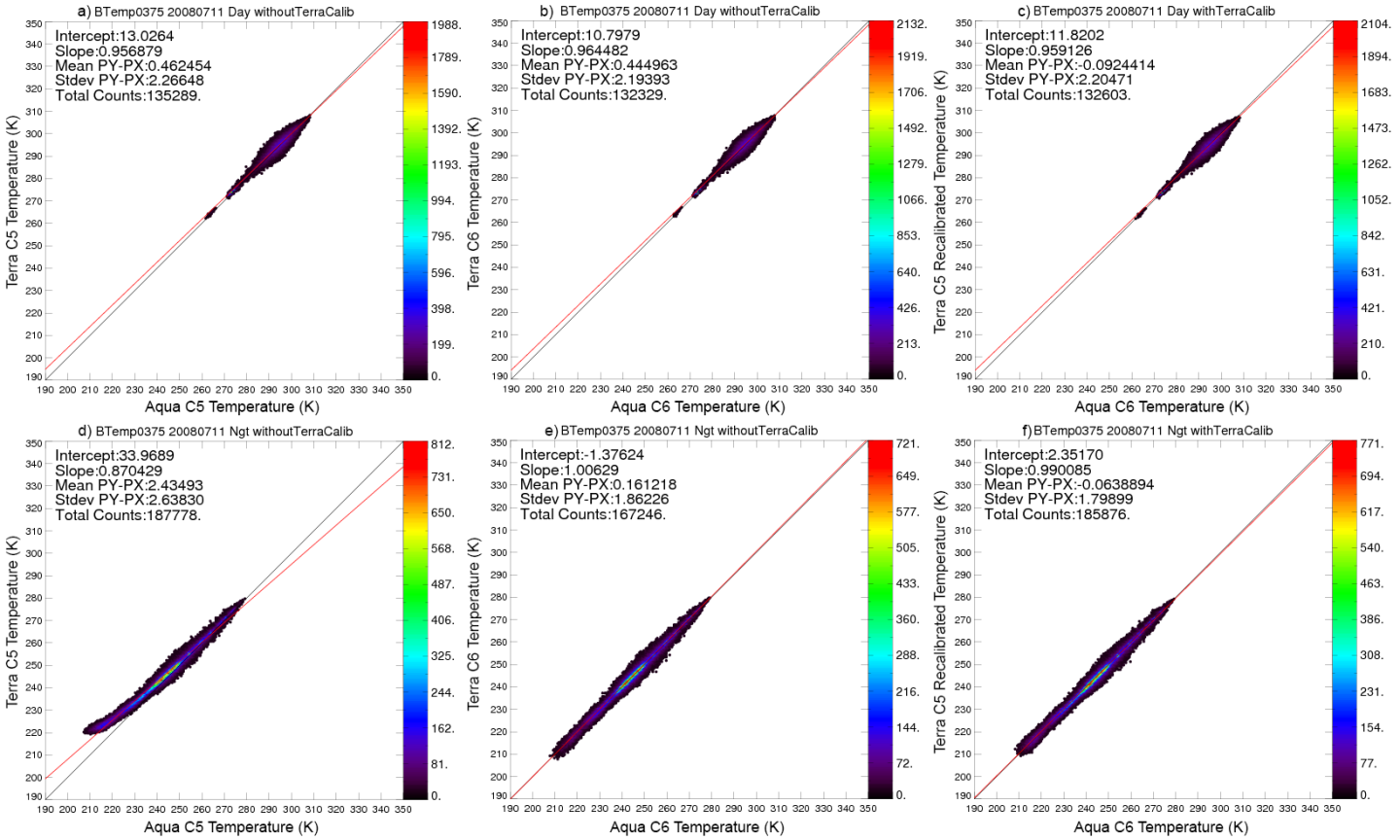

Figure 3. Same as Figure 2, except for shortwave infrared (3.8 µm) brightness temperature comparisons. Top – daytime, bottom (night).

The calibration adjustments described above yield results that are comparable to those developed for the MODIS C6 radiances. Figure 2 shows the scatterplots of matched Aqua and Terra for Channel 1 (0.65 µm) data taken 11 July 2008. Before applying the correction (Figure 2a), the Terra C5 reflectances were systematiically less than Aqua by 2% or less. The C6 calibrations (Figure 2b) rectified the differences, on average, while the CERES correction to Terra C5 data brought the differences to 0.005 in the mean, but yield excellent consistency with the line of agreement. On other days, the corrected Terra C5 data show better agreement with the Aqua C6 data than do the Terra C6 data. In general, though they yield essentially the same statistics, the corrected C5 Terra data typically show the better agreement with the 1:1 line relative to Aqua C6 data. The Aqua C6 and C5 data are nearly identical.

Similarly, the changes in the Terra C5 SIR channel calibration results in much greater consistency between Terra and Aqua. Figure 3 shows comparisons of matched Terra and Aqua Ch-20 brightness temperature data for day (top) and night (bottom), 11 July 2008. During the day, the original C5 temperatures (Figure 3a) differ by ~0.5 K as reported by Minnis et al. (2008b). The C6 data (Figure 3b) yield nearly the same mean difference $T_{Te} - T_{aq}$ suggesting that the Terra calibration changed little for C6 over the observed range. The CERES adjustment applied to the C5 data during the daytime (Figure 3a) reduces $|T_{Te} - T_{aq}|$ to less than 0.1 K. At night, the Terra C5 temperatures (Figure 3d) asymptote at ~220 K while T_{Aq} values continue to less 210 K, as seen earlier. The C6 calibrations (Figure 3e) straighten the curve, resulting in much better agreement between Aqua and Terra at the low temperatures. Applying the CERES corrections to T_{Te} also result in excellent agreement with slightly smaller mean differences and standard deviations. Examination of the remainder of the 2003, 2008, and 2013 matched data, however, indicate that $T_{Te} - T_{aq}$ has a seasonal cycle ranging from ~1.4 K

to ~0.4 K for C5 data during the daytime. The peak occurs around January and the minimum around July. Since the correction applied during the day is a constant, the corrected differences retain this cycle, except with mean values of ~0.6K during the boreal winter and ~-0.1 K during the boreal summer. This seasonal variation is to be further researched.

The absolute mean differences between the Terra and Aqua 1.24-µm reflectances (not shown) were reduced from ~0.012 to less than 0.005 using the CERES correction. Very little change was found in the Terra C6 calibration, so the CERES corrections yield better consistency between the Terra and Aqua reflectances for this channel. The changes to the 2.13-µm channel were minor (not shown). The reflectance agreement between Terra and Aqua for this channel is better than ±0.01 for C5, corrected C5, and C6 data. Overall, the corrections applied by CERES to the Terra C5 data bring the Terra and Aqua radiances into much better agreement than for the original C5 data. The agreement is as good or better than the agreement between the C6 Terra and Aqua radiances. Recent analyses of the C5 and C6 data by Doelling et al. (2015) reveal that the Aqua VIS channel began degrading around 2008 and by 2012 its response had degraded by 1%. Thus, it is likely that after 2008, some slight trends in the Aqua products, particularly the cloud optical depth, could become apparent.

Scene Identification (Scene-ID) or Cloud Mask

Based on these radiances, each MODIS pixel is classified as clear, cloudy, bad data, or no retrieval. Each clear or cloudy pixel is categorized as weak or strong indicating the degree of confidence. Clear pixels can have an additional classifier: snow, aerosol, smoke, fire, glint, or shadow. Cloudy pixels can also have a glint sub-classification meaning that they were detected at angles favorable for the viewing of specular reflection from the surface. Atmospheric profiles of temperature, ozone, and humidity, model estimates of surface emissivities and skin temperature, elevation, water percentage, ice/snow cover, and one of the 18 surface types (CERES Surface Type IDs) are also associated with each MODIS pixel. Because of problems with Aqua MODIS channel 6 (1.64 µm), channel 7 (2.13 µm) is being used in its place in both Terra and Aqua cloud detections. This substitution is especially critical for the ice/snow detection. The following remarks summarize changes in the cloud mask for Ed4 relative to the scene-ID methods used for Aqua Edition 1A and Terra Edition 2 (both hereafter referred to as Ed2).

- Daytime non-polar
    - Improved sun-glint detection in clear areas.
    - Improved sun-glint detection in cloudy areas.
    - Improved clouds, aerosol, and glint detection.
    - Improved cloud detections between dust and low clouds with added test of reflectance ratio, 1.24µm/0.65µm.
    - Improved thin cirrus detection over both ocean and land using 1.38-µm reflectance
    - Improved coastal cloud detection.
- Nighttime non-polar
    - Improved thin cirrus and low clouds detection
    - Increased cloud detection over ocean
    - Increased desert cloud detection by reducing the clear sky 3.75 - 11 µm brightness temperature difference (BTD) standard deviation from 2.0 to 1.5 K.
- Daytime Polar
    - Improved ice clouds, snow surface, clear land, thin cirrus detection.
    - Added a clear-snow ID by overwriting strong and weak-clear by using snow, ice, IGBP maps and spectral tests.
- Nighttime Polar
    - Improved inversion cloud detection.
    - Changed the cloudy thresholds over super cold plateau (Antarctica and Greenland).
    - Improved the classification of to-be-determined (TBD) pixels.
    - Added clear-sky-restore tests developed by MODIS team.
- Twilight Polar: Improved twilight polar tests
- Polar/non-polar lines are minimized.

Cloud Property Retrievals

The following values are computed for each cloudy pixel: phase (ice or water), VIS optical depth (over snow-covered surfaces, NIR1 is used instead of the VIS channel), IR emissivity, liquid or ice water path *WP*, water droplet or ice crystal effective radius R_e at three wavelengths (3.7, 2.1 and 1.24 µm), cloud-top, effective and base pressure (p_t p_c and p_b respectively), cloud-top, effective and base height (Z_t, Z_c and Z_b respectively), cloud-top, effective and base temperature (T_t, T_c and T_b respectively), cloud-top height (pressure and temperature) from CO_2 slicing retrieval Z_{CO2} (P_{CO2} and T_{CO2}), multilayer (ML) identification, upper-layer (UL) cloud-top height (pressure and temperature), upper-layer effective ice crystal radius R_e at two wavelengths (3.7 and2.1 µm), lower-layer (LL) cloud-top height (pressure and temperature), lower-layer effective water droplet radius R_e at two wavelengths (3.7 and 2.1 µm). While all

Table 2. Single pixel parameters saved for each MODIS pixel and provided along with other variables for construction of SSF.

Latitude, longitude (°)	CO2-slicing cloud top altitude, Z_{CO2} (km)
Solar zenith angle, SZA (°)	CO2-slicing multilayer upper cloud top altitude, Z_{UL} (km)
Viewing zenith angle, VZA (°)	CO2-slicing multilayer lower cloud top altitude, Z_{LL} (km)
Relative azimuth angle, RAA (°)	CO2-slicing multilayer upper cloud ice R_e: R_{UL} (µm)
MODIS channel 1 and 7 reflectances: ρ_1, ρ_7	CO2-slicing multilayer lower cloud water R_e: R_{LL} (µm)
MODIS channel 20, 31, and 32 temperatures: T_{20}, T_{31}, T_{32} (K)	CO2-slicing multilayer upper cloud optical depth: τ_{UL}
Cloud droplet or ice crystal effective radius at 3.8 µm, R_e (µm)	CO2-slicing multilayer lower cloud optical depth: τ_{LL}
Cloud optical depth, τ	CO2-slicing multilayer detection index
Cloud water path (gm^{-2})	BTD (11-12 µm) multilayer detection index
Cloud effective, top, and base altitude, Z_e, Z_t, Z_b (km)	Pavolonis multilayer detection index
Cloud effective temperature, T_e (K)	IGBP surface type (1-18)
Cloud Mask Value	Snow map index (0 = no snow; 1 = snow)
Cloud Mask Clear Category	Ice map percentage (%)
Cloud Mask Cloud Category	SINT_VISST flag
Cloud Particle Phase	Cloud droplet/ice crystal effective radius at 1.24 µm, R_e (µm)
	Cloud droplet/ice crystal effective radius at 2.13 µm, R_e (µm)

parameters are given a value or retain a default value and may be used in the construction of the SSF, individual pixel values are retained for the parameters listed in Table 2. These are saved for use in validation and other analyses of cloud properties. No values are assigned to cloudy pixels having no retrievals. No properties could be retrieved for 1.0 and 5.8% of the detected cloudy pixels over ocean and land, respectively, during the day for a total of 2.2%, a decrease from 4.0% for Ed2. At night, the number of no retrievals drops to 0.4% of the total number of pixels classified as cloudy.

Normally, the cloud phase, temperature, effective particle size and optical depth are computed using the VIS-IR-SIR-SWC Technique (VISST), which matches model estimates of radiances from clouds with the observations (Minnis et al. 2011). The VIS channel is primarily used to estimate τ, the IR channel is for T_c, the SIR channel is used for the particle size, and the SWC is used to help the phase selection. Cloud height and pressure are found by matching T_c to an altitude in Global Modeling and Assimilation Office (GMAO) Goddard Earth Observing System Model Version 5.4.1 (GMAO-G541) vertical profile of temperature for the pixel location and time. If the underlying surface is determined to be snow- or ice-covered either from the snow-ice maps or from identification of nearby pixels as clear snow, then the SIR-IR- NIR1 Technique (SINT) is applied (Minnis et al. 2011). The SINT uses NIR1 as the channel to compute the VIS optical depth. All ice crystal reflectance lookup tables (LUT) for the 0.6, 3.7, 2.1, and 1.2 µ channels used in Ed4 are based on radiative transfer computations using hexagonal ice columns with roughened surfaces having the normalized roughness parameter set equal to 1 (Yang et al. 2008). Ed2 used smooth hexagonal ice columns (Minnis et al., 1998). The water droplet reflectance LUTs used in Ed4 are the same as those in Ed2 (Minnis et al. 1998), except that new LUTs were computed for the 1.24 and 2.1-µm channels using the same approach as that in Minnis et al. (1998). Corrections for atmospheric absorption use radiative transfer calculations, as in Minnis et al. (2011), employing the correlated *k*-distribution method (Kratz, 1995) with the absorption coefficients computed for the spectral response functions of the various channels.

In previous editions, boundary-layer cloud height was calculated with a constant lapse rate, 7.1 K / km (Minnis et al. 2011). Ed4 uses regional monthly mean apparent lapse rates map over ice-free water, snow-free land, and snow-covered surfaces respectively for both daytime and nighttime. Sun-Mack et al. (2014) describe how this lapse rate is applied in conjunction with the GEOS-5 temperature profile. Examples of daytime seasonal lapse rate global maps over snow/ice free scenes are shown in Figure 4, where DJF denotes for winter, MAM spring, JJA summer and SON fall. The monthly lapse rates used in Ed4 result from interpolation of two adjacent seasons.

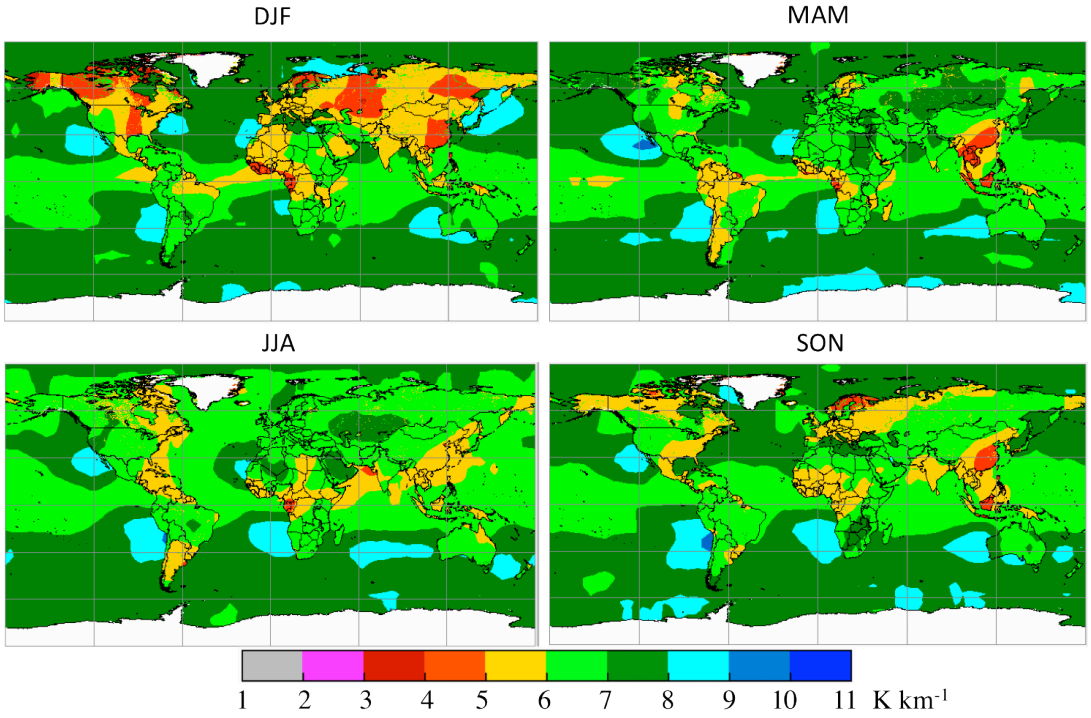

Figure 4. Daytime boundary layer lapse rates (K km^{-1}) over snow/ice-free scenes for winter (DJF), spring (MAM), summer (JJA), and fall (SON). From *Sun-Mack et al*. (2014).

Standard Cloud Parameters

The Ed4 validation relies on direct comparisons of Ed4 cloud properties with ground truth data and other satellites, consistency between Aqua and Terra, as well as on comparisons with Ed2 results, which have been compared more extensively with ground truth data. Assessment of the uncertainties in some of the cloud parameters has been completed for the Ed4 results from those comparisons. Many other datasets must be compared with the CERES MODIS cloud analyses before final error numbers are assigned. The cloud parameters have also been evaluated visually by comparing a large number of high-resolution images with pictures of derived cloud products over a selected number of regions to ensure that the results appear to be qualitatively consistent with the imagery. Some of the parameters have been compared with climatological values to obtain a rough quantitative evaluation. The results have also been averaged for various surface types and angular ranges to determine any systematic variability. The most quantitative evaluations use estimates of similar quantities derived from passive and active radiometric measurements at surface sites, the CALIPSO lidar products, CloudSat radar products, and liquid water path from the AMSR-E microwave radiometer. The available ARM data have been compared with the VIRS Ed2, Terra Ed2, GOES-8 using the CERES VISST algorithm, and with Aqua Ed2 properties (see TRMM Edition2A and Terra Edition2A Cloud Properties Accuracy and Validation Sections) and are documented in several papers (e.g., Mace et al. 2005). Some comparisons with Ed2 datasets are discussed below. The results are similar to those found applying the CERES algorithm to GOES-8 data (Mace et al. 1998; Dong et al. 2002; Min et al. 2004, Xi et al. 2014). It will not be possible to evaluate trends in the Ed4 data until at least 10 years of data are processed.

Inter-platform consistency and changes relative to Ed2

Cloud amount:

The primary changes to the cloud mask were to increase daytime thin Ci detection for ocean and land, better aerosol (heavy dust) and low cloud discrimination in the Atlantic Ocean, increased nighttime thin Ci and low clouds detection for ocean and land, improved polar cloud and snow/ice detection, and smoother transitions into polar regions. Currently there are ~15 years (2000 – 2014) of Terra Ed2 (same cloud retrieval version in all of Terra Ed2A, Ed2B, Ed2F, Ed2G, and Ed3A), ~12 years (2002 – 2014) of Aqua Ed2 (same cloud retrieval version in all of Aqua Ed2A, Ed2B, Ed2C, Ed2D, and Ed3A), ~7 years (2000 – 2007) of Terra Ed4 and ~5 years (2002 – 2007) of Aqua Ed4. Figure 5 shows the time series of daytime cloud amount over non-polar ocean (Figure 5a), non-polar land (Figure 5b), polar ocean (Figure 5c) and polar land (Figure 5d). Each plot in Figure 5 has 4 different time series, Aqua Ed2 (cyan), Aqua Ed4

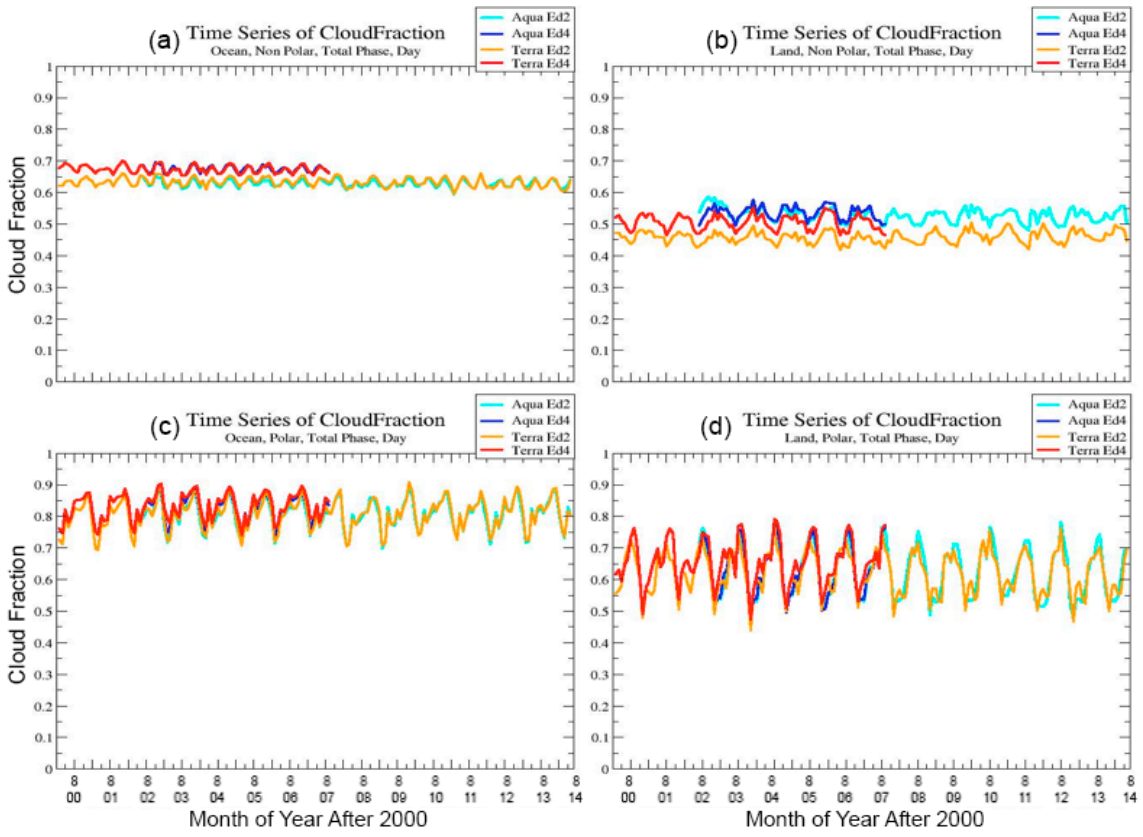

Figure 5. Time-series of daytime cloud amount over (a) non-polar ocean, (b) non-polar land, (c) polar ocean, and (d) polar land). Each plot has 4 different time-series, Aqua Ed2 (cyan), Aqua Ed4 (blue), Terra Ed2 (orange) and Terra Ed4 (red).

(blue), Terra Ed2 (orange) and Terra Ed4 (red). The mean daytime Aqua and Terra Ed4 cloud amounts over nonpolar ocean are nearly identical and nearly 0.05 greater than their Ed2 counterparts. Over nonpolar land areas, the Terra cloud fraction increased by ~0.05 relative to the Ed2 means, drawing closer to the Aqua Ed4 means, which are slightly greater than their Ed2 values. The Aqua and Terra Ed4 mean cloud fractions over the polar land and ocean are very consistent and differ only slightly from the Ed2 averages.

Figure 6 plots the same parameters as Figure 5, except for nighttime. The mean nonpolar marine cloud amounts (Figure 6a) increased by 0.05 - 0.10 from Ed2 to Ed4. The Aqua Ed4 values are slightly greater than those from Terra unlike those found for Ed2. Similarly, the Ed4 cloud fractions over nonpolar land (Figure 6b) are ~0.08 greater than the Ed2 means, with slightly greater values form Terra compared to Aqua. The Ed4 cloud fractions over nighttime polar ocean (Figure 6c) are more than 0.10 greater than their Ed2 counterparts and generally very consistent across platform. Over polar land (Figure 6d), the nighttime Ed4 cloud amounts from Terra and Aqua are nearly the same, while the Ed2 Terra means are ~0.05 and 0.04 greater than the Ed4 and Aqua Ed2 values, respectively.

Table 3 summarizes the global mean cloud amounts from all Ed2 and Ed4 data currently available at ASDC (Aqua Ed2: 2002-2014, Terra Ed2: 2000-2014, Aqua Ed4: 2002-2007, Terra Ed4: 2000-2007). Overall during daytime, globally, Aqua (Terra) Ed4A picks up additional 0.03 (0.04) of clouds over the corresponding Ed2 averages. At night, the additional clouds detected by Edition4A are 0.09 for Aqua and 0.07 for Terra compared to Ed2.

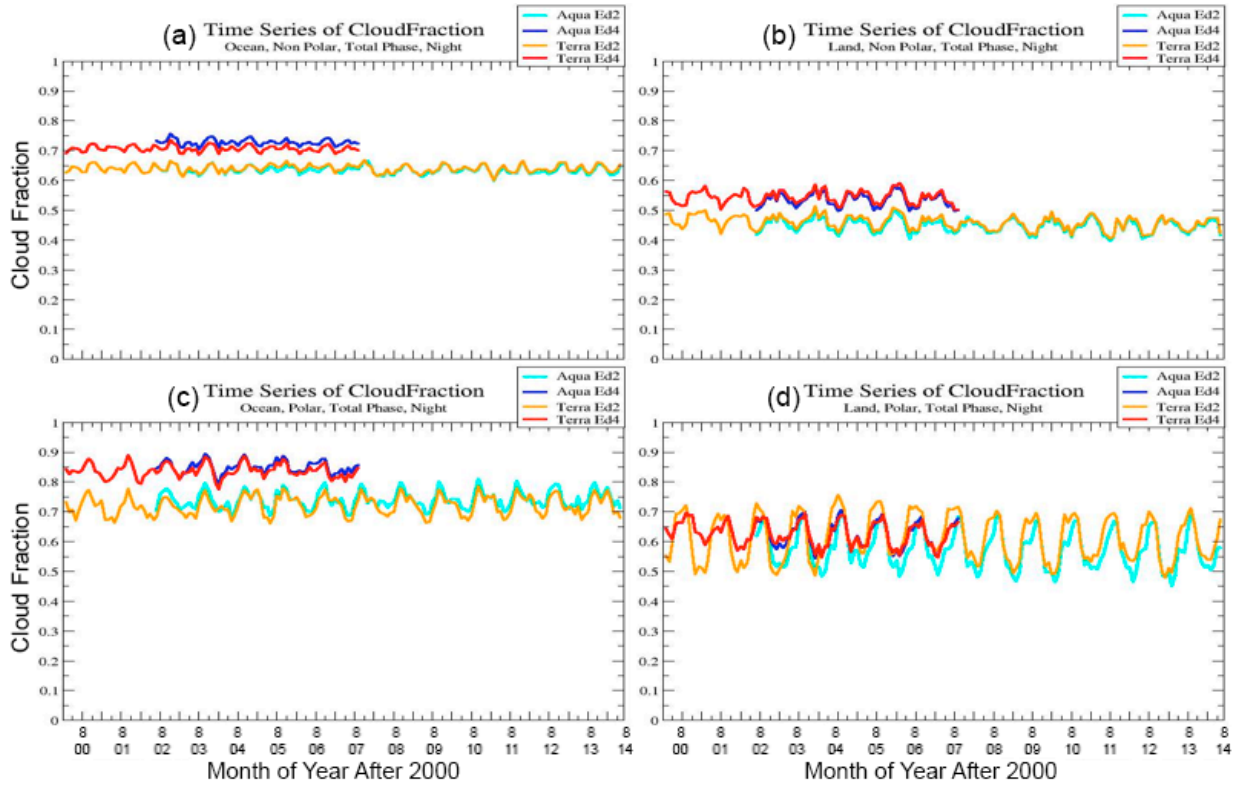

Figure 6. Same as Figure 5, but for nighttime.

Cloud phase:

Cloud phase statistics changed significantly from Ed2 to Ed4 as shown in the mean liquid water cloud fraction in Table 4 and in Figure 7 and Figure 8, which plot time series of day time and nighttime water cloud fractions, respectively, for the same cloud datasets used for Figure 5 and Figure 6. The water cloud fraction is defined here as the fraction of the total cloud cover that is determined to be liquid water clouds. Thus, the water and ice cloud fractions should add up to 1.0. During daytime, the water fraction increased for both satellites in Ed4 over nonpolar ocean (Figure 7a), especially for the Aqua analysis. Water cloud fraction increased by ~0.15 over nonpolar land (Figure 7b) for Ed4 relative to Ed2. Similar increases are apparent over polar ocean (Figure 7c) and somewhat smaller increases over polar land (Figure 7d). Overall, the Ed4 Terra and Aqua daytime water cloud fractions are more consistent temporally than their Ed2 counterparts. The overall 0.08 water cloud increase balanced by a 0.08 ice cloud fraction decrease is mainly a result of a change in cloud phase determination that flagged many supercooled clouds as ice in Ed2. A decreasing trend in water cloud fraction starts around 2008 over polar regions during daytime for both Terra Ed2 and to a lesser extent for Aqua Ed4. Because it is primarily in the Terra data, it may be linked to the changes in the calibration and the switch from the GEOS-4 to GEOS-5 input data for Ed2 in January 2008. If so, then the trend should be greatly diminshed in the Ed4 data.

Table 3. Fractional mean cloud amounts, Aqua Ed2: 2002-2014, Terra Ed2: 2000-2014, Aqua Ed4: 2002-2007, Terra Ed4A: 2000-2007.

	Ocean			Land			Ocean & Land		
	Non-polar	Polar	Global	Non-polar	Polar	Global	Non-polar	Polar	Global
					Day				
Aqua (Ed2)	0.63	0.81	0.65	0.53	0.63	0.54	0.60	0.74	0.62
Terra (Ed2)	0.64	0.81	0.66	0.46	0.63	0.48	0.59	0.73	0.61
Aqua (Ed4)	0.68	0.83	0.69	0.54	0.64	0.55	0.64	0.75	0.65
Terra (Ed4)	0.68	0.84	0.69	0.51	0.66	0.53	0.63	0.76	0.65
					Night				
Aqua (Ed2)	0.64	0.75	0.65	0.45	0.58	0.47	0.59	0.67	0.60
Terra (Ed2)	0.65	0.73	0.66	0.46	0.62	0.48	0.60	0.69	0.61
Aqua (Ed4)	0.73	0.86	0.75	0.54	0.63	0.55	0.68	0.74	0.69
Terra (Ed4)	0.71	0.84	0.73	0.55	0.63	0.56	0.67	0.74	0.68

Table 4. Same as Table 3, except for water cloud amount as a fraction of total cloud cover.

	Ocean			Land			Ocean & Land		
	Non-polar	Polar	Global	Non-polar	Polar	Global	Non-polar	Polar	Global
					Day				
Aqua (Ed2)	0.58	0.55	0.58	0.46	0.39	0.45	0.55	0.48	0.54
Terra (Ed2)	0.64	0.56	0.63	0.47	0.36	0.46	0.60	0.46	0.58
Aqua (Ed4)	0.66	0.68	0.66	0.60	0.49	0.59	0.65	0.59	0.64
Terra (Ed4)	0.68	0.67	0.68	0.62	0.46	0.61	0.66	0.58	0.65
					Night				
Aqua (Ed2)	0.54	0.33	0.52	0.35	0.19	0.33	0.49	0.26	0.46
Terra (Ed2)	0.52	0.34	0.50	0.34	0.19	0.32	0.47	0.27	0.45
Aqua (Ed4)	0.62	0.50	0.60	0.42	0.26	0.40	0.57	0.38	0.55
Terra (Ed4)	0.60	0.49	0.59	0.42	0.25	0.40	0.56	0.37	0.53

At night (Figure 8), the Terra and Aqua water cloud fractions increased substantially, by 0.08 to 0.10, over all areas from Ed2 to Ed4. The inter-platform consistency is about same for nonpolar areas (Figure 8a, b). Over marine polar areas (Figure 8c), the consistency appears to be slightly worse in Ed4 with the Aqua fractions being a bit greater than Terra during some months, particularly the boreal summer when the southern ice pack is observed at night and parts of the Arctic ocean are in the terminator zone during some overpasses. The mean difference, however, is only 0.01. The agreement between Terra and Aqua Ed4 over land is very tight for all months.

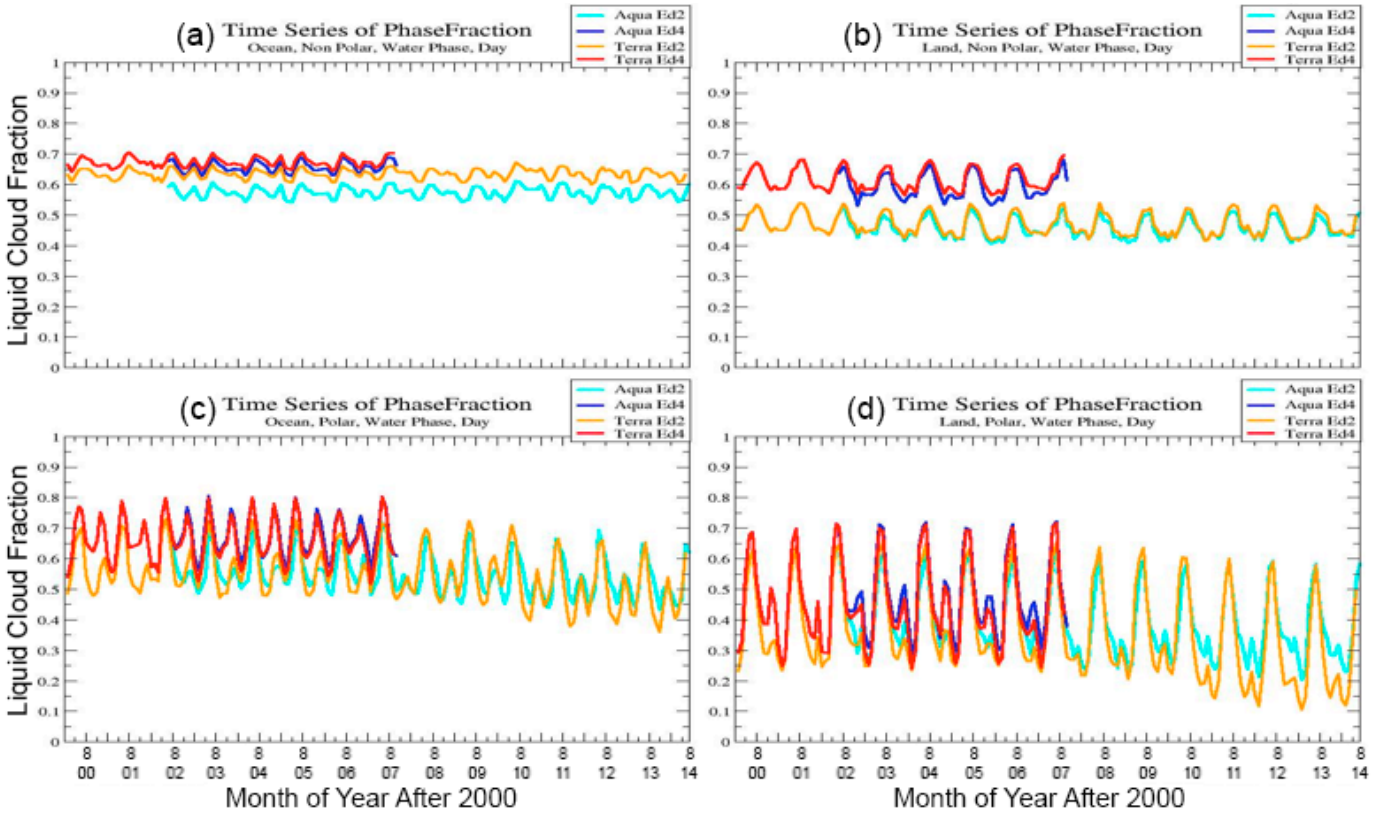

Figure 7. Same as Figure 5, except for liquid water cloud fraction.

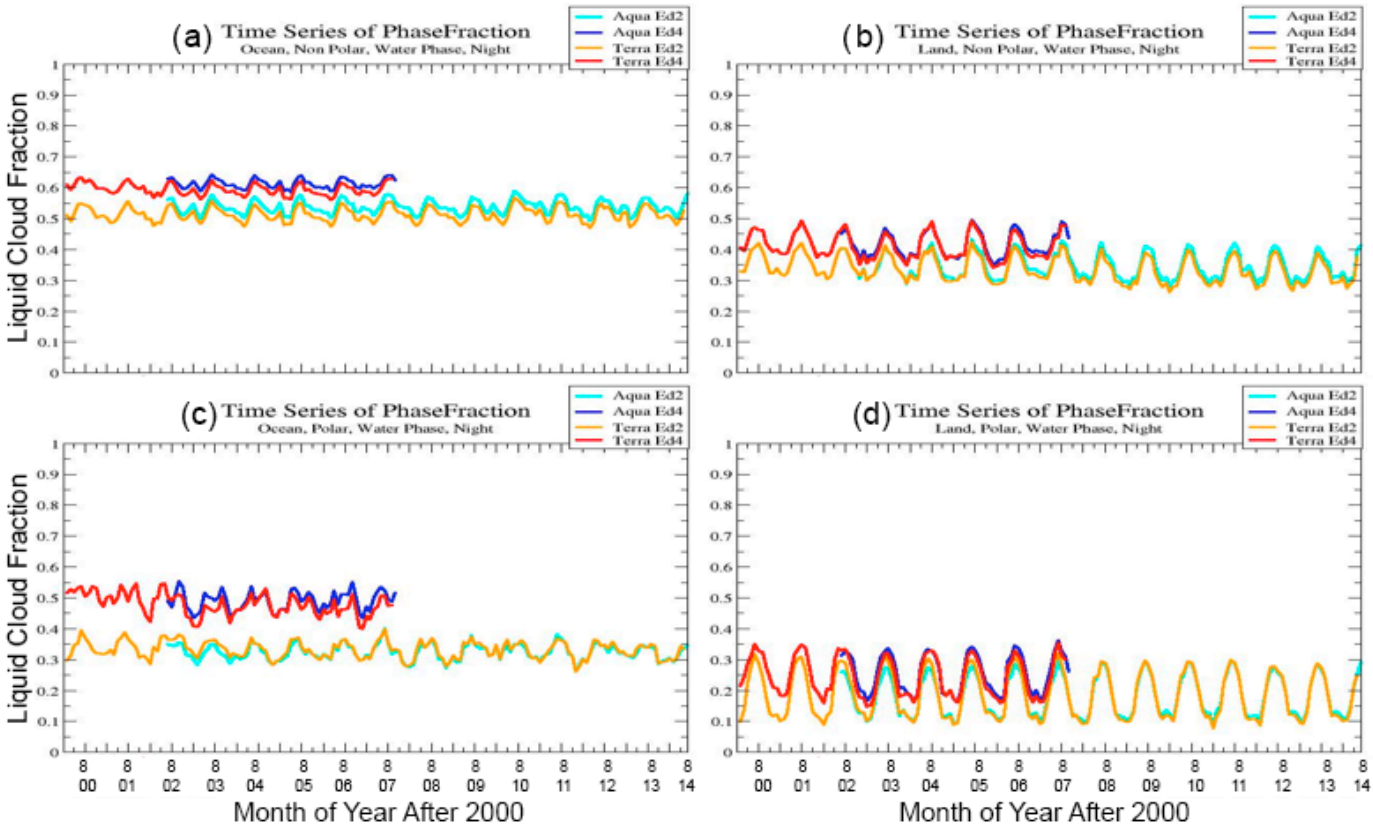

Figure 8. Same as Figure 5, but for nighttime.

Standard cloud height, pressure, and temperature

These parameters are all related because the cloud effective temperature T_e is used to ascertain cloud effective height Z_e and the height, in turn, is used to select the pressure. Effective cloud height derived from MODIS should be an altitude somewhere between the top and base of the cloud. It corresponds to the mean radiating temperature of the cloud. For water clouds, the level of T_e is usually within a few 100 m of the top. For cirrus clouds, it can be close to the cloud base or near cloud top depending on the density of the cloud. For simplicity, the physical cloud top height Z_t for water clouds is assumed to be the same as the effective height, while for optically thin ice clouds, it is determined as a function of T_e and τ or cloud emissivity (Minnis et al. 2011). In Ed2, it was assumed for optically thick ice clouds that Z_t is constrained to be below the tropopause and to correspond to a temperature differing from T_e by no more than 2 K (Minnis et al. 2011). For Ed4, the tropopause constraint was removed and a new parameterization based on the results of Minnis et al. (2008c) was assumed to be implemented. However, a coding error, in many instances, overwrote the results of the new parameterization in the final version of Ed4 and, thus, the new parameterization has to be applied by the user to get the expected results. The impact of using the parameterization is demonstrated in the next section. If the phase is ice, $\tau \geq 6.0$, and $Z_e >$ 4.2 km, then the following parameterization should be applied to the data *ex post facto*.

$$Z_t = \{Z_e + [(0.751 + 0.094*Z_e)* \cos(\mathrm{VZA})]\} * corrfac, \quad (2)$$

where VZA is the viewing zenith angle and all heights are in km, all heights are in km, and when $Z_e > 6$ km and < 13 km,

$$corrfac = 0.453 + Z_e * (0.1737 + Z_e * (0.000519*Z_e - 0.01687)). \quad (3)$$

If Z_e is below the tropopause height, then Z_t is constrained to be less than or equal to the tropopause height.

An additional cloud-top height estimation method is applied when the pixel is determined to correspond to an overshooting cloud top according to the method of Bedka et al. (2010). In that instance, if $T_e < T_{trop}$, then $Z_t = Z_{trop} +(T_{trop} - T_e)/8$.

Cloud base height Z_b is estimated the difference between Z_t and cloud thickness ΔZ. The latter is estimated based on T_e, τ, and cloud phase using various empirical formulae. For ice clouds, the method described by Minnis et al. (2010) is used. For water clouds,

$$\Delta Z = 0.3896 * \ln(\tau) - 0.0101. \quad (4)$$

This parameterization is based on the matched satellite and surface data reported by Chakrapani et al. (2002). If $\tau < 1.03$,

$$\Delta Z = 0.085\ \tau^{1/2}, \quad (5)$$

the old parameterization from Ed2.

Time series of the daytime mean Ed2 and Ed4 cloud effective heights are presented in Figure 9 and Figure 10 for liquid water and ice clouds, respectively, for the same datasets used for Figure 5. The mean values day and night are summarized in Table 5. The Terra and Aqua daytime water cloud heights from Ed4 are remarkably consistent with each other, differing by no more than 0.1 km. This contrasts with the Ed2 Aqua means, which are noticeably smaller than their Terra counterparts, particularly over nonpolar areas (Figure 9a, b). This change from Ed2 to Ed4 is the result of the phase changes noted above. Over polar oceans (Figure 9c), the daytime Ed4 water clouds are generally higher than the Ed2 clouds, but over polar land, the Ed4 and Ed2 values are similar. Overall, the Aqua Ed4 daytime water cloud Z_e means exceed the corresponding Ed2 means by 0.52 km, compared to 0.13 km for Terra. At night (bottom, Table 5), the Ed4 changes raised Z_e by 0.15 and 0.55 km over nonpolar and polar ocean areas, respectively, above their Ed2 counterparts. Over land, the mean Z_e for water clouds dropped by 0.1 km over nonpolar areas, but Ed4 increased Z_e by 0.8 km in the polar regions.

While the Ed4 daytime ice cloud heights (Figure 10) are generally more consistent than their Ed2 predecessors, the seasonal swings over nonpolar regions (Figure 10a, b) exceed those for Ed2. In the polar regions (Figure 10c, Figure 10d), the Ed4 Aqua and Terra means are nearly identical, unlike their Ed2 counterparts, which have distinct differences. On average, daytime ice cloud height from Terra rose from 7.5 km (Ed2) to 8.87 km (Ed4), a change of 1.37 km, while for Aqua, Z_e increased from 7.8 km to 9.04 km, a boost of 1.26 km (see

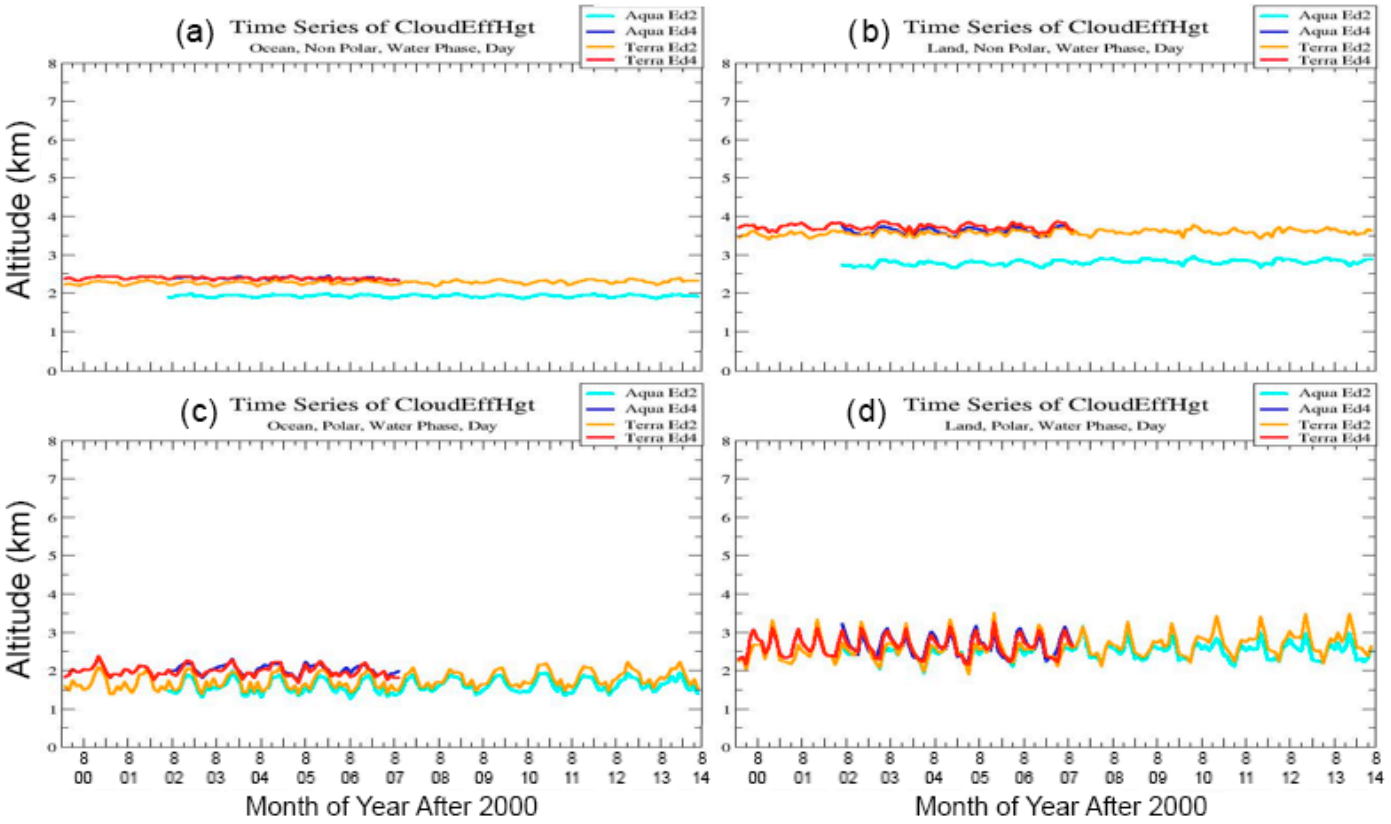

Figure 9. Same as Figure 3, except for daytime water cloud effective height.

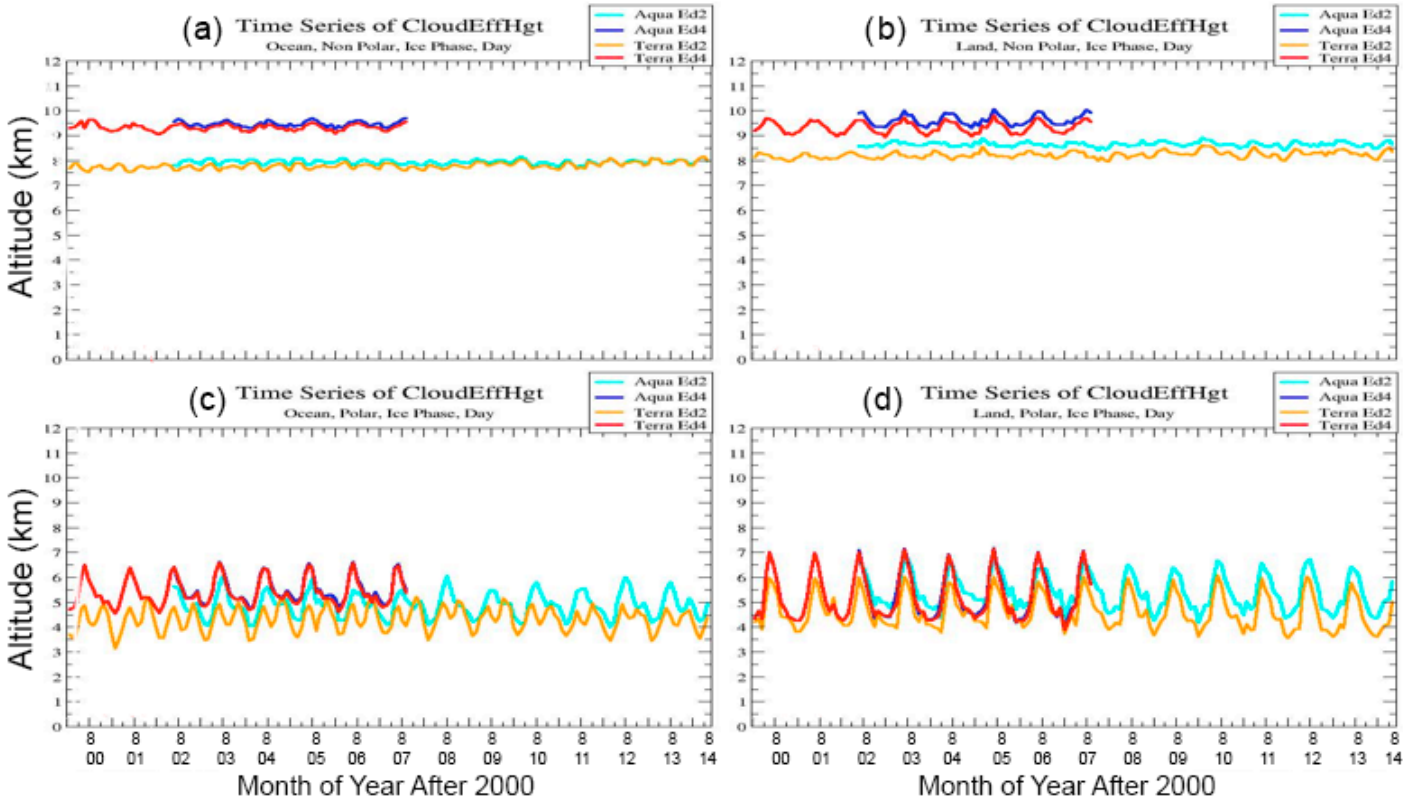

Figure 10. Same as Figure 9, but for ice clouds.

Table 5). At night over ocean and land (Table 3), the mean increase in cloud heights for Ed4 are ~0.8 and 0.9 km, respectively. The increased ice cloud heights for Ed4 can be attributed to several factors. These include the implementation of a CO_2 slicing algorithm (see subsection below) and a new ice crystal reflectance model in Ed4, as well as the reclassification of some lower ice clouds in Ed2 as liquid clouds in Ed4, The daytime Aqua ice cloud heights over non-polar regions are 0.29 and 0.14 km higher than Terra for Ed4, over land and ocean, respectively. These differences flip at night, when the Ed4 Aqua ice cloud mean heights are 0.28 and 0.20 lower than the Terra values over ocean and land, respectively. This day-night switch could reflect diurnal changes in the cloud properties.

Standard daytime cloud optical depth, effective particle size based on 3.8-µm channel

Time series of Terra and Aqua Ed2 and Ed4 mean water and ice cloud optical depths are shown in Figure 11 and Figure 12, respectively. The long-term mean values are summarized in Table 6. On average, Ed4 τ means for both nonpolar ice and water clouds from Aqua are slightly greater than than those from Terra over land (Figure 11b and Figure 12b) and vice versa over ocean (Figure 11a and Figure 12a). This difference is likely due to distinct systematic diurnal changes over the two surfaces, Overall, the nonpolar Ed4 retrievals yield somewhat larger optical depths than their Ed2 counterparts, ~0.4 for water clouds and ~0.5 for ice clouds (Table 6). Unlike the Ed2 results, the ice and water cloud optical depths from Terra and Aqua are very consistent over the polar regions (Figure 11c, d; Figure 12c, d). Moreover, the Ed4 polar means are significantly elevated relative to their Ed2 counterparts by 5 and 10 for ice and water clouds, respectively. These increases are partly caused by the use of different NIR channels in the Ed2 and Ed4 algorithms over snow and ice surfaces and secondarily by the use of different parameterizations. Over snow-covered surfaces, the SINT algorithm used the 1.6 and 2.13-µm channels in Ed2 to derive optical depth for Terra and Aqua, respectively, and used only the 1.24-µm channel in Ed4 for both satellites. The maximum retrievable τ for the Ed2 NIR channels is much smaller than that for 1.24 µm. Thus, much of the difference between Ed2 and Ed4 over polar regions is a result of the switch in the NIR channels. Mean optical depth over polar areas is nearly twice that of non-polar region, and in Ed4 has larger (smaller) seasonal fluctuations for liquid (ice) clouds compared to those in Ed2.

Examination of the polar optical depths seasonally reveals that the greatest Ed4-Ed2 differences are found during fall and winter when the solar zenith angles (SZAs) are greatest and they are reduced during spring and fall when the average SZAs are smaller. For example during fall 2004, the mean Terra Ed4 Arctic (65 – 90°N) water (ice) cloud τ is ~26 (19) compared to ~15 (9) for Ed2. The

Table 5. Same as Table 3, except for mean cloud effective height (km).

	Day								
	Ocean			Land			Ocean & Land		
	Non-polar	Polar	Global	Non-polar	Polar	Global	Non-polar	Polar	Global
Water									
Aqua (Ed2)	1.93	1.62	1.90	2.81	2.53	2.78	2.17	2.02	2.15
Terra (Ed2)	2.28	1.74	2.23	3.58	2.63	3.49	2.62	2.14	2.57
Aqua (Ed4)	2.39	2.03	2.35	3.62	2.66	3.53	2.72	2.32	2.67
Terra (Ed4)	2.39	1.99	2.35	3.73	2.65	3.63	2.75	2.31	2.70
Ice									
Aqua (Ed2)	7.95	4.89	7.64	8.65	5.41	8.35	8.09	5.08	7.78
Terra (Ed2)	7.80	4.32	7.45	8.23	4.62	7.90	7.87	4.41	7.50
Aqua (Ed4)	9.48	5.52	9.08	9.63	5.29	9.23	9.47	5.38	9.04
Terra (Ed4)	9.34	5.41	8.94	9.34	5.24	8.96	9.29	5.31	8.87
	Night								
	Ocean			Land			Ocean & Land		
	Non-polar	Polar	Global	Non-polar	Polar	Global	Non-polar	Polar	Global
Water									
Aqua(Ed2)	2.59	1.17	2.42	4.19	1.71	3.90	3.00	1.41	2.79
Terra(Ed2)	2.59	1.15	2.42	4.14	1.66	3.85	3.00	1.37	2.78
Aqua(Ed4)	2.72	1.72	2.60	4.06	2.52	3.88	3.06	2.11	2.94
Terra(Ed4)	2.75	1.69	2.63	4.01	2.48	3.83	3.08	2.07	2.95
Ice									
Aqua(Ed2)	9.34	3.88	8.67	9.67	4.49	9.07	9.37	4.13	8.69
Terra(Ed2)	9.40	3.86	8.72	9.83	4.65	9.22	9.46	4.21	8.77
Aqua(Ed4)	9.96	5.32	9.39	10.54	5.47	9.95	10.07	5.37	9.45
Terra(Ed4)	10.24	5.25	9.63	10.74	5.41	10.12	10.33	5.30	9.67

differences for Aqua are even greater, given that Aqua Ed2 uses the 2.13-µm channel. The Aqua Ed4 Arctic water (ice) cloud τ is ~25 (19) compared to ~11 (6) for Ed2. The differences are even greater during winter. During spring 2004, when snow/ice cover was quite high, the mean Terra Ed4 Arctic water (ice) cloud τ is ~16 (9) compared to ~11 (6) for Ed2. The corresponding Aqua Ed2 water and ice τ means are ~9 and ~5, respectively. Similar results are seen during the summer months when more areas are free of snow and ice. This seasonal variation is also seen in the Antarctic. Because the extremely large optical depths seen in Ed4 occur at times of high SZA over the Arctic, it is likely that the plane-parallel-based parameterization of 1.24-µm reflectance is unable to properly characterize the SZA-dependence of the reflectance fields over snow similar to the findings of Loeb and Coakley (1998) for VIS-channel retrievals of stratocumulus τ over ocean. The Ed2 results are not as extreme during the winter and fall probably because of the maximum limits on the retrievals at the 1.6 and 2.1-µm wavelengths. Better understanding of the uncertainties in retrievals over snow will require comparisons with independent datasets that are less dependent on SZA and plane-parallel theory.

Time series of mean 3.8-µm liquid droplet and ice crystal effective radii are plotted in Figure 13 and Figure 14, respectively, and their averages are listed in Table 7. In all cases, the Ed4 droplet r_e averages from Aqua are almost the same as those from Terra, differing by 0.1 µm or less. The corresponding Ed2 Aqua means are 0.4 µm greater than those from Terra. The reduced difference in Ed4 is due to the normalized 3.8-µm calibrations. The Aqua and Terra Ed2 and Ed4 r_e means track each other temporally quite closely (Figure 13), however, the average values over nonpolar ocean and land rose by 0.2 and 1.1 µm from Ed2 to Ed4. The reflectance models for water clouds are identical for editions. This difference is likely due to changes in the liquid water cloud fraction and in the temperature and humidity profiles.

For Ed2, ice cloud particle size was given as effective diameter defined as in Ou et al. (1993). For Ed4, effective radius is used for ice clouds and is defined in the same manner as the droplet effective radius. That is, it is the radius computed for a sphere having the same solid volume as the ice crystal. To compare Ed2 and Ed4 ice particle sizes, ice effective diameter was converted to radius. The

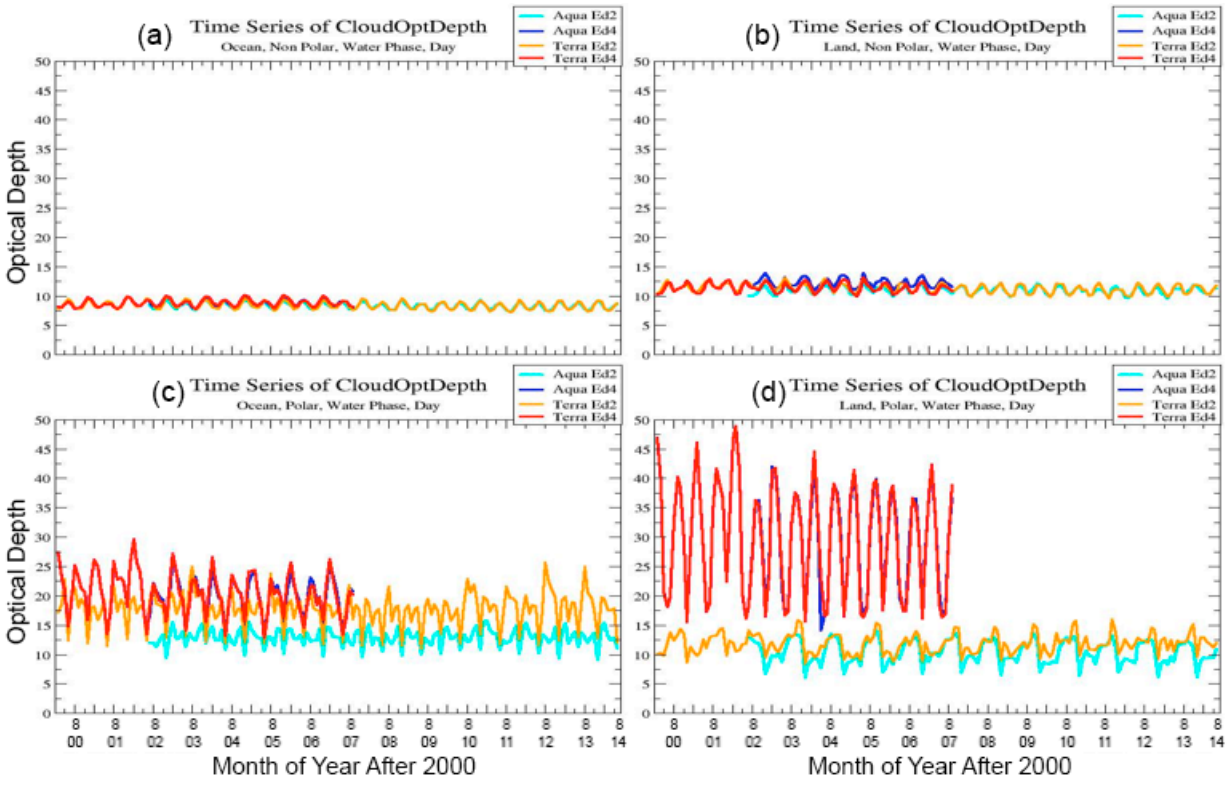

Figure 11. Same as Figure 5, except for daytime water cloud optical depth.

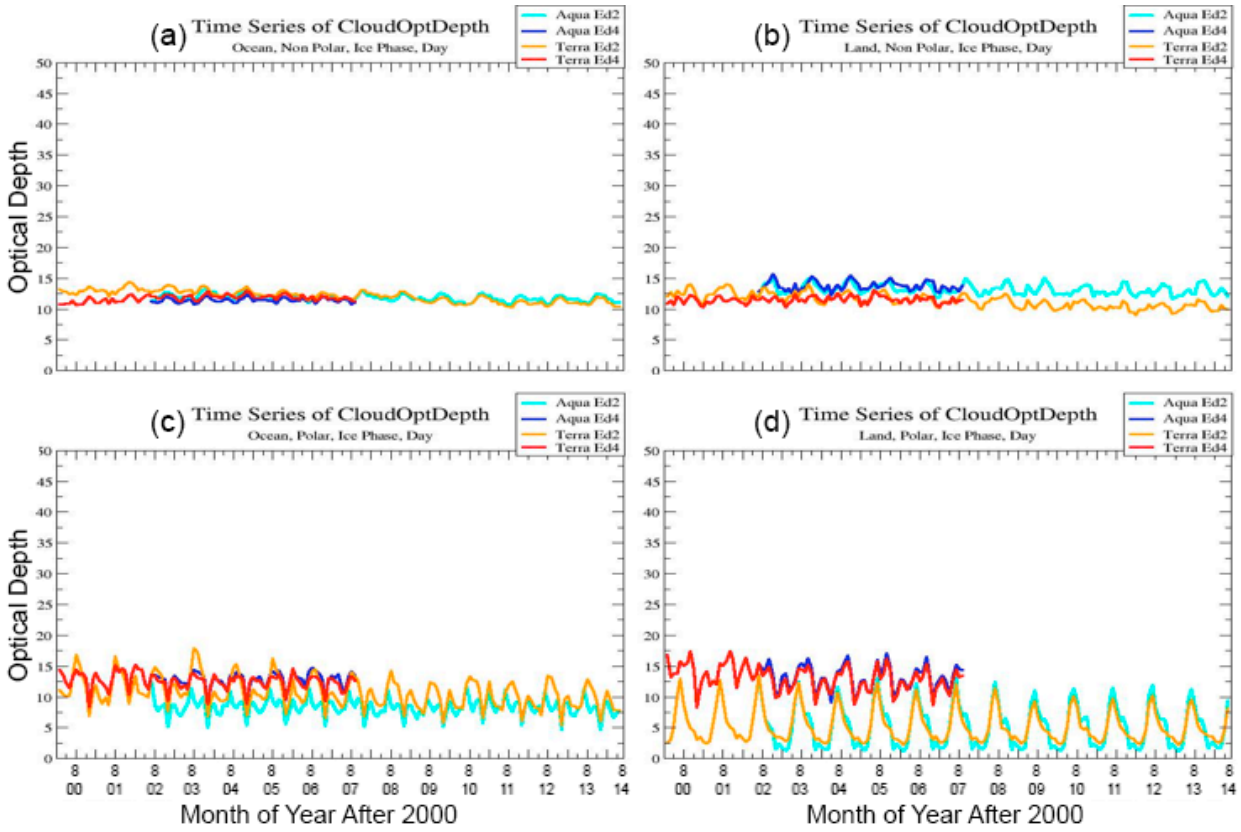

Figure 12. Same as Figure 11, except for daytime ice cloud optical depth.

Table 6. Same as Table 3, except for daytime mean cloud optical depths.

	Ocean			Land			Ocean & Land		
	Non-polar	Polar	Global	Non-polar	Polar	Global	Non-polar	Polar	Global
Water Clouds									
Aqua (Ed2)	8.33	12.92	8.80	10.98	10.47	10.96	8.97	11.84	9.29
Terra (Ed2)	8.44	17.70	9.40	11.32	11.89	11.39	9.17	15.64	9.88
Aqua (Ed4)	8.79	20.03	9.97	12.27	28.79	13.97	9.67	23.59	11.24
Terra (Ed4)	8.84	20.53	10.07	11.44	29.75	13.32	9.51	24.19	11.18
Ice Clouds									
Aqua (Ed2)	11.87	8.37	11.53	13.19	5.23	12.44	12.04	7.07	11.50
Terra (Ed2)	12.12	10.71	12.01	11.39	5.31	10.81	11.82	8.45	11.47
Aqua (Ed4)	11.43	12.77	11.59	13.76	13.17	13.73	11.91	12.81	12.02
Terra (Ed4)	11.78	12.56	11.88	11.50	13.10	11.67	11.60	12.59	11.72

time series of mean ice crystal r_e for both Ed2 and Ed4 (Figure 14) show excellent coherence over all surfaces, however, the Ed2 Terra means significantly exceed their Aqua counterparts everywhere, except over nonpolar land. There is very little difference between Terra and Aqua Ed4 ice r_e everywhere, except over land, where a diurnal effect may be operative. Over nonpolar ocean, the Ed4 means are only ~0.5 (~2) µm smaller than the Aqua (Terra) Ed2 values despite the differences in ice crystal models. Over all other areas, the Ed4 means are greater than the corresponding Ed2 averages (Table 7). This is especially evident over the polar regions. Again the larger difference over the polar regions is mainly caused by larger optical depth retrieved using the 1.24-µm channel. It is clearly seen that Aqua and Terra Ed4 are consistent for both water and ice clouds, ocean and land, and polar and non-polar.

Despite similarities in the time series, the Ed4 mean values of re for ice clouds are probably better representations of the ice crystal sizes than found for Ed2. It is expected that ice crystal size will be positively correlated with temperature, such that larger crystals are found at higher temperatures. Figure 15 shows scatterplots of zonal mean r_e for Ed2 (Figure 15a) and Ed4 (Figure 15b) versus zonal mean T_e. It is clear that there is no relationship between r_e and T_e in the Ed2 means, while the two parameters are highly correlated in the Ed4 results over land and water surfaces. If the land and ocean means are considered together, the squared linear correlation coefficient R^2 increases to 0.76 (not shown). Thus, it is concluded that the Ed4 ice crystal effective size is a marked improvement over that retrieved for Ed2.

Table 8 shows mean liquid and ice water path from both Ed2 and Ed4 for cloudy pixels only. To obtain the total LWP or IWP, the results would need to be multiplied by the cloud fraction. Here, cloud water path CWP is computed as

$$CWP = 0.67\, r_e\, \tau, \qquad (6)$$

assuming that the retrieved effective size is representative of the cloud as a whole. Alternatively, LWP can be estimated adiabatically by multiplying the result of Eq(6) by 0.83 (Bennartz 2007). Overall for non-polar regions, the Ed4 Aqua (Terra) LWP is 15% (12%) greater than that for Ed2, while the Ed4 Aqua (Terra) IWP is 2% (8%) smaller. Over polar regions, CWP from Ed4 is about twice that of Ed2 due to larger Ed4 optical depths .

Table 7. Same as Table 3, except for daytime mean cloud droplet radius and ice crystal effective radius (µm).

	Ocean			Land			Ocean & Land		
	Non-polar	Polar	Global	Non-polar	Polar	Global	Non-polar	Polar	Global
Water Cloud									
Aqua (Ed2)	14.3	12.5	14.1	10.7	12.6	10.9	13.4	12.6	13.3
Terra (Ed2)	13.9	12.5	13.8	10.4	12.4	10.4	13.0	12.4	12.9
Aqua(Ed4)	14.4	12.6	14.2	11.7	12.5	11.8	13.7	12.6	13.6
Terra (Ed4)	14.5	12.6	14.3	11.6	12.5	11.7	13.7	12.5	13.7
Ice Cloud									
Aqua (Ed2)	25.2	23.5	25.1	21.7	26.0	22.1	24.3	24.8	24.4
Terra (Ed2)	26.9	26.9	26.9	21.3	28.5	22.0	25.5	27.6	25.8
Aqua (Ed4)	24.7	34.7	25.7	23.6	35.6	24.7	24.5	35.3	25.7
Terra (Ed4)	24.9	34.5	25.9	23.1	35.4	24.3	24.5	35.1	25.7

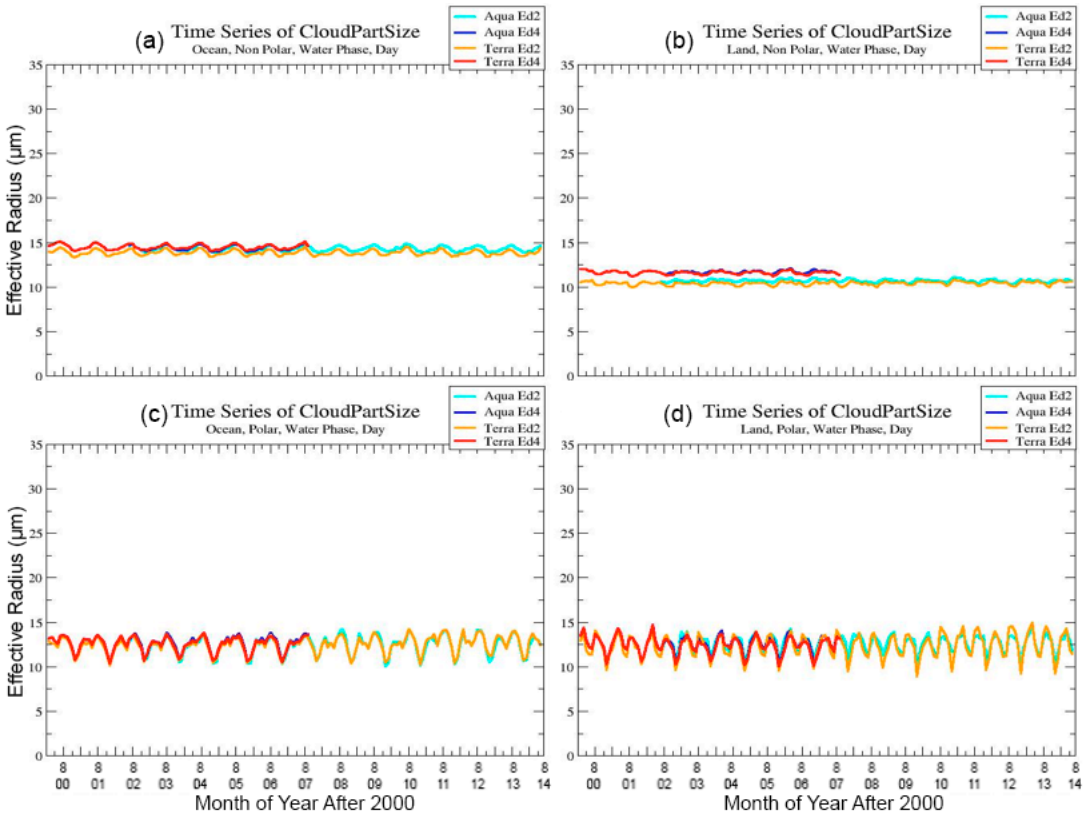

Figure 13. Same as Figure 11, except for daytime liquid cloud radii.

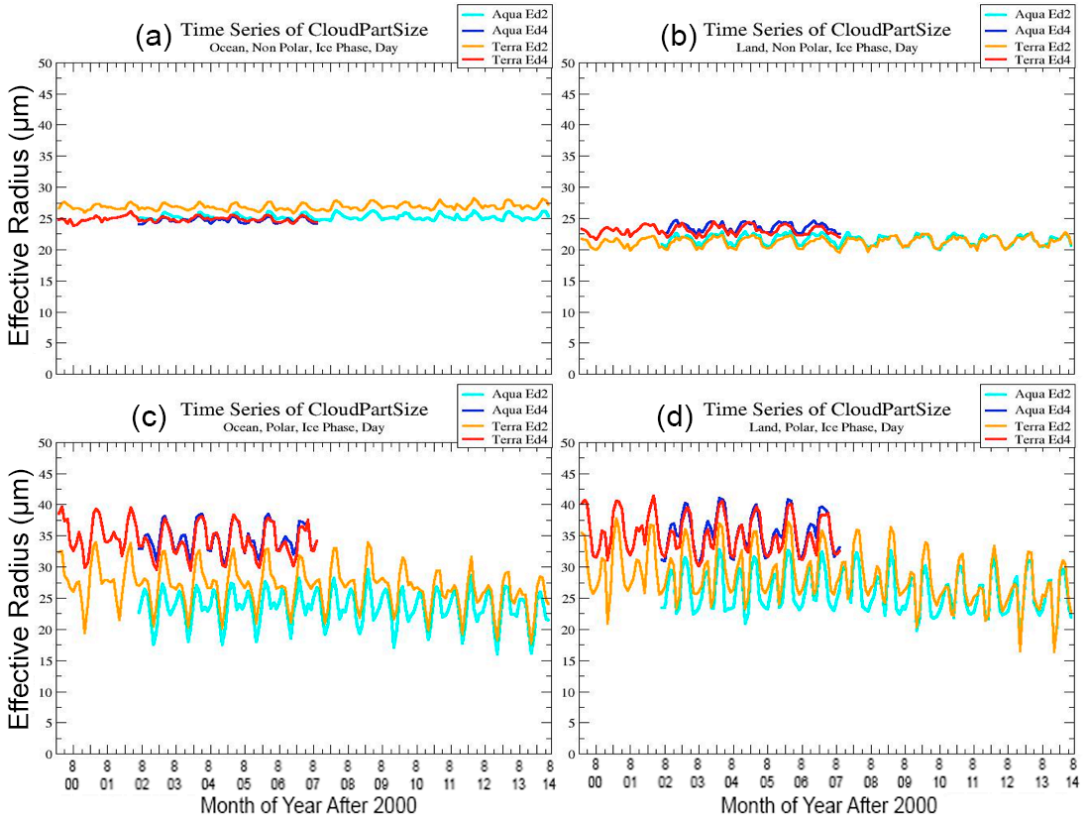

Figure 14. Same as Figure 13, but for ice cloud.

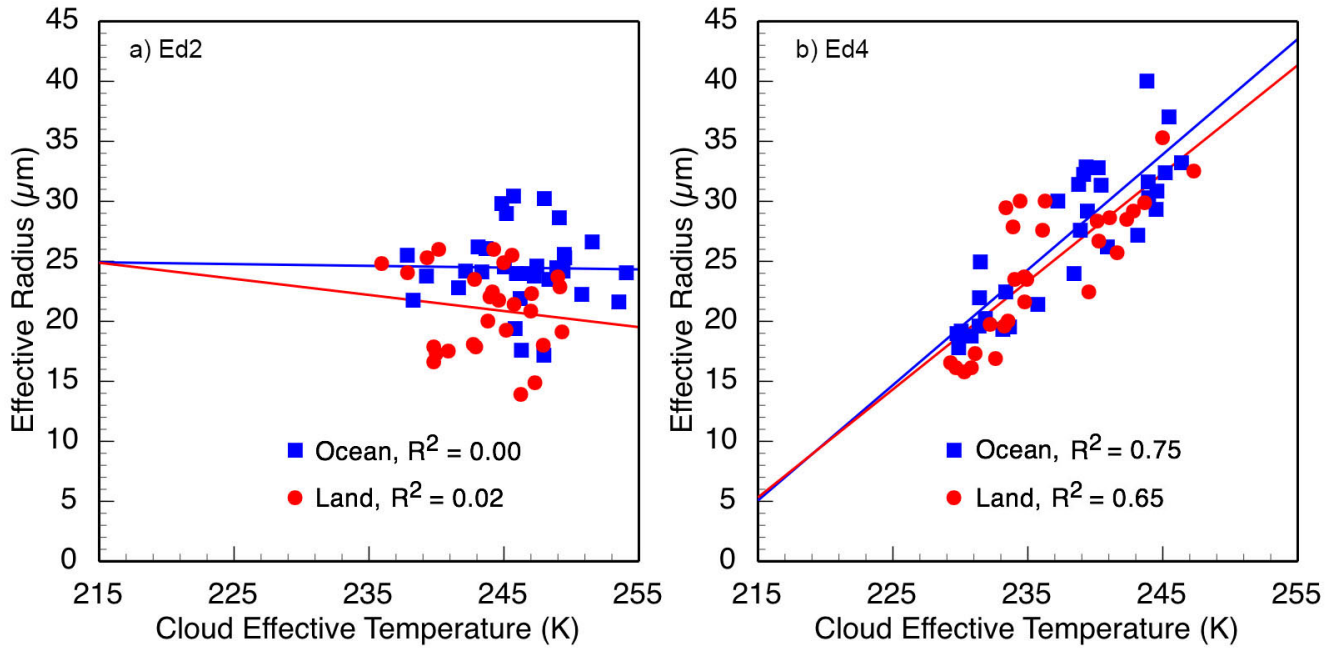

Figure 15. Correlation of zonal mean cloud ice crystal effective radius and mean cloud effective temperature, July 2013.

Non-standard cloud particle size retrievals (Ed4 only)

Figure 16 shows the time-series of daytime liquid and ice cloud r_e derived from 3 different channels over non-polar ocean (top), and non-polar land (bottom). The solid and dashed lines represent water and ice clouds, respectively. The standard retrievals using 3.8 μm radiances are indicated with blue (cyan) lines for Aqua (Terra). The non-standard 2.1-μm retrievals are shown as dark green (light green) lines for Aqua (Terra), while the non-standard 1.24-μm sizes are denoted with red (orange) lines for Aqua (Terra). The jump in the Terra 1.24-μm r_e values around June 2003 is due to the 14 May 2003 implementation of the Terra calibration adjustments. It appears that the Terra 1.24-μm calibration adjustment resulted in overestimates of r_e relative to Aqua, except for non-polar land for ice clouds. Table 9 shows the daytime mean cloud droplet radius and general ice effective radius for Aqua Ed4 (2002-2007) and Terra Ed4 (2000-2007). It is clearly seen from Figure 16 and the results in Table 9 that r_e averages from 2.13 and 1.24 μm are significantly greater than the standard means based on 3.8 μm. Some differences are expected for r_e retrieved from the three channels. However, the magnitudes of the differences are far beyond expectations, except for the water cloud results from 2.13-μm. After the Ed4 software was released, it was found that some of the retrieval model parameters were input in reverse order and affected primarily the retrievals of r_e for ice clouds using 2.13 and 1.24 μm and for water clouds using 1.24 μm. The impact is explored further in the validation section below. The upshot of the analyses is that **r_e from the 1.24-μm channel should not be used** in any case and that the **2.13-μm values of r_e should not be used for ice clouds.** The programming errors will be corrected in the next edition for CERES.

Table 8. Same as Table 3, except for daytime mean liquid and ice cloud water-path (gm^{-2}) over cloudy areas only.

	Ocean			Land			Ocean & Land		
	Non-polar	Polar	Global	Non-polar	Polar	Global	Non-polar	Polar	Global
Water Cloud									
Aqua (Ed2)	75.9	98.6	78.3	76.4	79.2	77.0	75.4	90.2	77.2
Terra (Ed2)	76.3	143.5	83.4	78.2	88.4	79.4	76.4	125.2	81.9
Aqua (Ed4)	82.9	195.2	95.0	97.7	353.0	124.5	86.5	260.5	106.6
Terra (Ed4)	83.4	199.8	96.0	92.0	362.1	120.1	85.4	263.3	106.0
Ice Cloud									
Aqua (Ed2)	214.0	127.8	205.6	208.6	80.5	196.6	209.4	107.8	198.6
Terra (Ed2)	234.3	173.9	228.8	180.5	83.1	171.2	218.1	135.2	209.5
Aqua (Ed4)	199.8	229.3	203.3	227.9	256.4	231.0	205.2	240.7	209.3
Terra (Ed4)	207.6	220.7	209.4	190.6	253.8	197.1	201.4	232.0	205.1

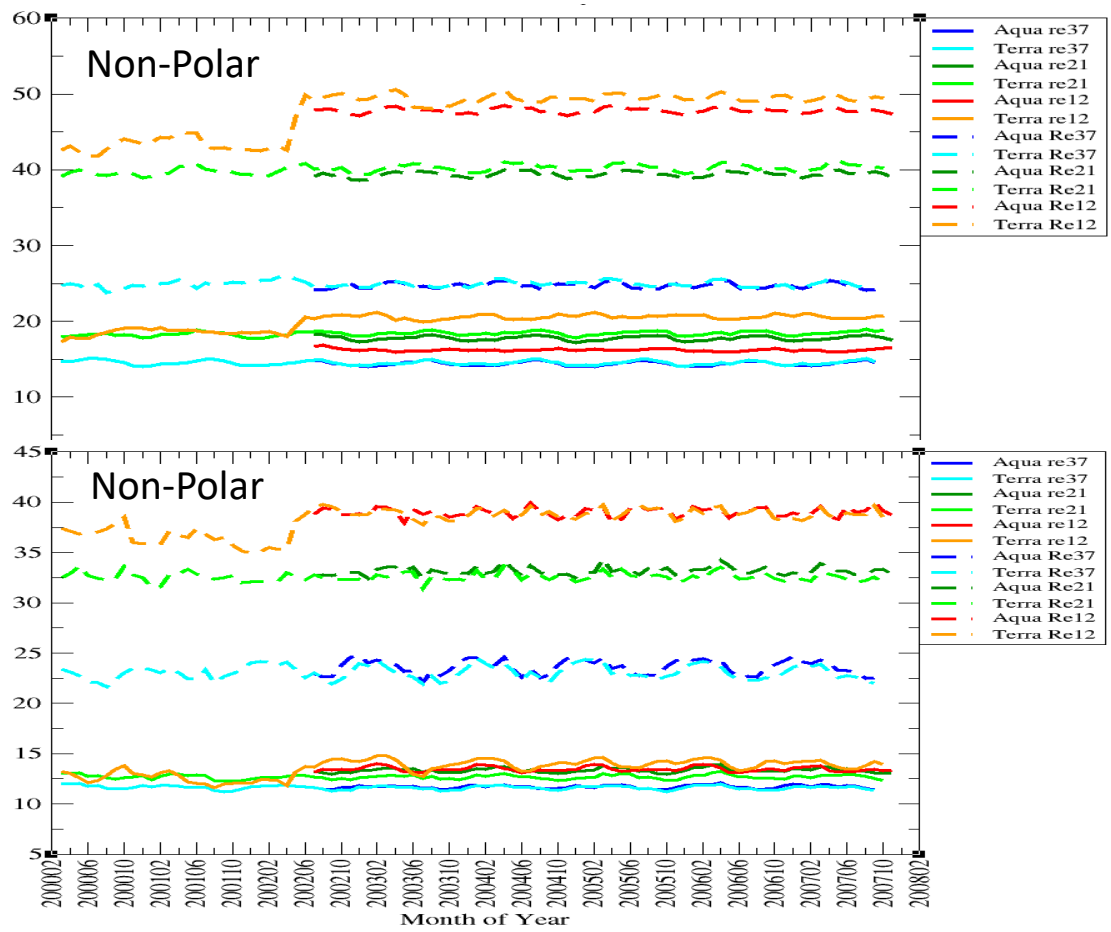

Figure 16. Time-series of Ed4 daytime liquid and ice cloud radii retrieved using 3.7 µm for Aqua (blue) and Terra (cyan), 2.1 µm for Aqua (dark green) and Terra (light green), 1.24 µm for Aqua (red) and Terra (orange) over non-polar ocean (top) and land (bottom). Solid lines represent water clouds and dashed lines, ice clouds. Aqua Ed4: 2002-2007; Terra Ed4: 2000-2007.

Table 9. Daytime mean cloud droplet and ice crystal effective radius from 3.8, 2.13, and 1.24 µm retrievals. Aqua Ed4: 2002-2007; Terra Ed4: 2000-2007.

	Ocean			Land			Ocean & Land		
	Non-polar	Polar	Global	Non-polar	Polar	Global	Non-polar	Polar	Global
Water Clouds									
Aqua (3.8)	14.4	12.6	14.3	11.7	12.5	11.8	13.7	12.6	13.6
Terra (3.8)	14.5	12.6	14.3	11.6	12.5	11.7	13.8	12.5	13.7
Aqua (2.13)	17.8	14.0	17.4	13.3	13.5	13.4	16.6	13.7	16.3
Terra (2.13)	18.4	14.1	18.0	12.7	13.7	12.8	16.9	13.9	16.6
Aqua (1.24)	16.2	17.3	16.3	13.5	16.9	13.7	15.5	17.0	15.7
Terra (1.24)	20.0	18.3	19.8	13.6	17.1	13.9	18.3	17.6	18.3
Ice Clouds									
Aqua (3.8)	24.7	34.7	25.7	23.6	35.6	24.7	24.5	35.3	25.7
Terra (3.8)	24.9	34.5	25.9	23.1	35.4	24.3	24.5	35.1	25.7
Aqua (2.13)	39.4	40.2	39.5	33.1	38.1	33.5	37.9	39.5	38.0
Terra (2.13)	40.1	40.2	40.1	32.6	38.6	33.0	38.3	39.6	38.4
Aqua (1.24)	47.8	48.8	47.9	39.0	51.1	39.9	45.6	48.4	45.9
Terra (1.24)	47.7	47.7	47.7	38.2	50.3	39.1	45.3	47.4	45.5

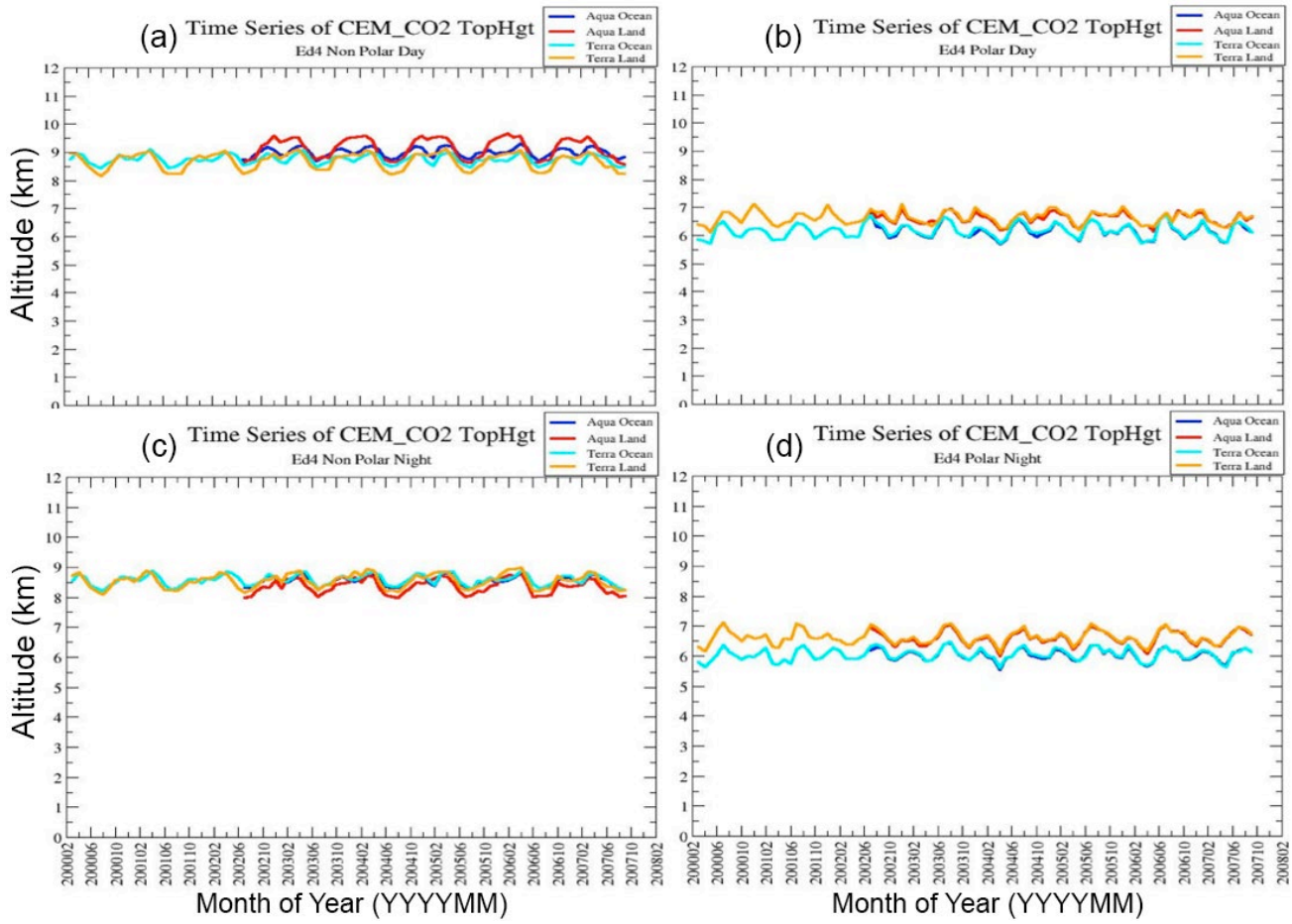

Figure 17. Mean Ed4 CO_2-emission cloud top heights during daytime (top) and nighttime (bottom) over non-polar (left) and polar (right) regions from Aqua over ocean (blue) and land (red) and Terra over ocean (cyan) and land (orange). Aqua Ed4: 2002-2007; Terra Ed4: 2000-2007.

CO_2 absorption cloud top height (Ed4 only):

An alternative cloud height is provided for high clouds in Ed4 retrieved with the CO_2-emission method (CEM) as developed by Chang et al. (2010) using only two spectral channels, 11.0 and 13.3 µm, to infer cloud top height for the highest cloud whether for single- or multilayered conditions. It differs from the traditional CO_2 slicing methods (e.g., Smith and Platt, 1978; Wylie and Menzel, 1999; Menzel et al. 2008) **i**n that it solves for the cloud top radiating temperature using estimates for the effective background radiances, instead of using the clear-sky background radiances for the solution. Because the new approach utilizes the Terra and Aqua MODIS 11.0 and 13.3-µm, it has the potential for improving the inference of the upper troposphere transmissive cloud properties in both single- and multilayer situations at relatively high temporal and spatial resolutions. This height is only retained when the CEM-retrieved pressure is less than 0.62 times the surface pressure. Otherwise, no value is given for CEM in the results.

Figure 17 shows the time series of the mean CERES Terra and Aqua CEM cloud top heights for polar and nonpolar regions through 2007. The results are seasonally coherent, but some differences in magnitude are evident. Over nonpolar land, the Aqua CEM height peaks during the day (Figure 17a) and yields the lowest values at night (Figure 17c) in contrast to the Terra results. A smaller day-night change is evident over ocean. These variations are reasonable given our knowledge of the diurnal cycles of convection. Over polar regions, the CEM heights are greater over land both day (Figure 17c) and night (Figure 17d). But there is no significant difference between the Terra and Aqua results. The polar CEM heights exceed the Z_e means for ice clouds (Table 5), but over nonpolar areas, the CEM heights are slightly lower than their ice cloud counterparts in Table 5. This suggests that the CEM retrievals include some liquid phase clouds in nonpolar regions. Overall, the inter-platform consistency is excellent and the heights are reasonable.

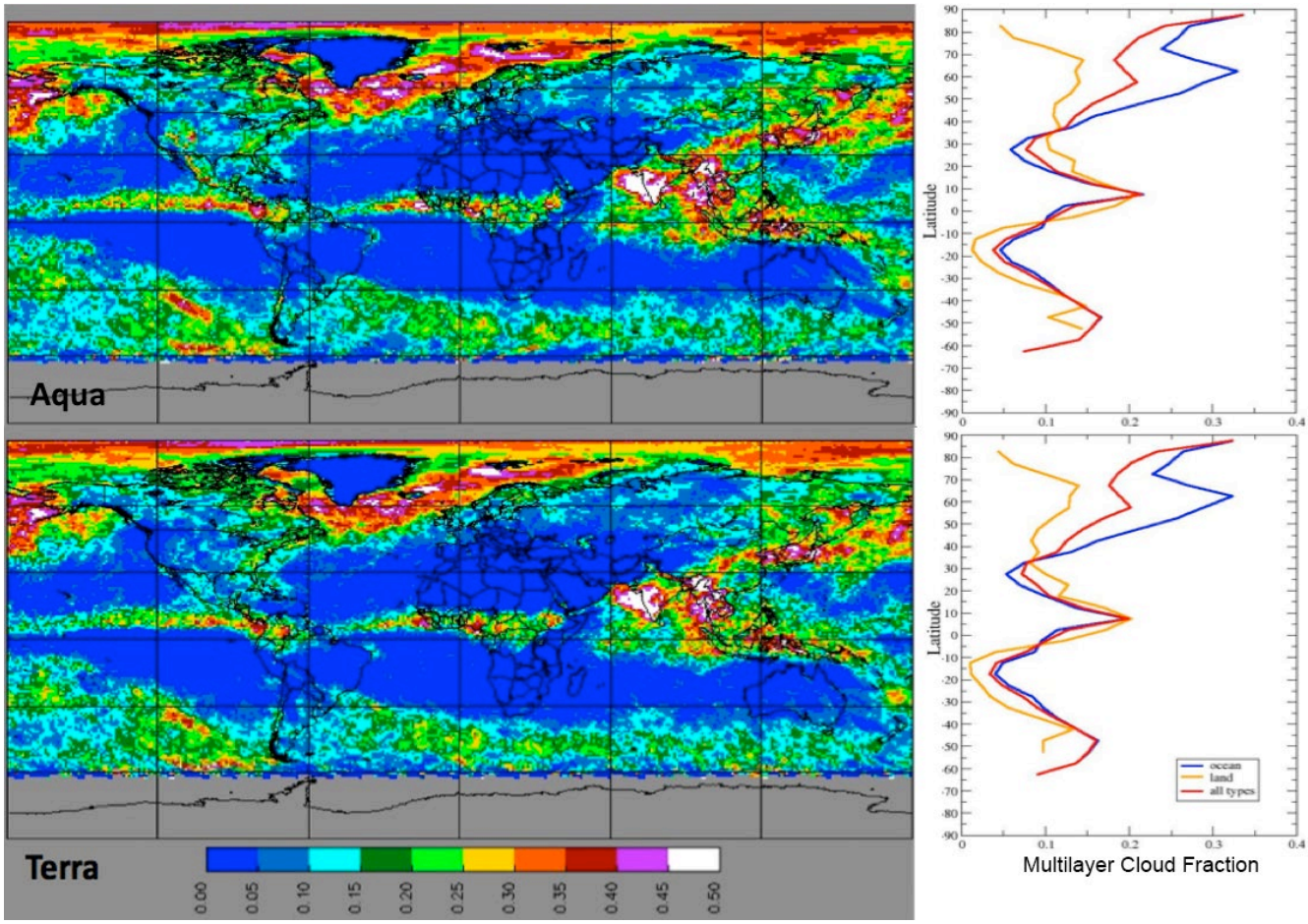

Figure 18. Daytime multilayer cloud fraction from Aqua (top) and Terra Ed4 (bottom), July 2013.

Multilayer cloud fraction and layer properties (Ed4 only):

The multilayer algorithm to identify ice clouds over water clouds is applied to every cloudy MODIS pixel and returns a flag indicating that the pixel is multilayer cloud, convective or thick cloud, or single-layer (SL) cloud. Multilayer cloud fraction is calculated using the number of multilayer cloud pixels divided by the total number of pixels (including both clear and cloudy) in a grid box. Figure 18 shows the results of the algorithm applied to July 2013 Aqua and Terra daytime MODIS data. Here, the grid has a 10' resolution. The figure shows that multilayer cloud fractions are greatest over the Northern Hemisphere storm tracks and the intertropical convergence zones. The Aqua and Terra results are very consistent in this figure and in Figure 19, which shows time series of multilayer cloud fraction for the available period. No trends are evident in any of the panels. Mean multilayer cloud fractions for polar and non-polar ocean and land areas are summarized in Table 10, which indicates more multilayer clouds over ocean (16% day & night) in the polar region than over land (6% daytime, 7% nighttime). On average, the multilayer cloud fraction is 12% (day & night) over non-polar region. It is noted that detecting multilayered clouds over snow and ice is more uncertain than detection over darker surfaces.

Retrievals of upper and lower layer cloud top heights and microphysical properties are performed for each pixel identified as multilayered. The time series in Figure 20 indicate that the upper and lower layer cloud heights retrieved from Aqua and Terra data are very consistent and show no trends. Both the upper and lower heights over land exceed those over ocean in all areas day and night. Over nonpolar regions, the Aqua upper-layer clouds are slightly higher than those from Terra, while the opposite is true at night. This day-night switch is likely a diurnal cycle effect. No differences are apparent between the two datasets over polar regions. The daytime averages in Table 11 for low clouds over ocean are comparable to those for water clouds (Table 5). Over land, the

averages are lower than the corresponding water cloud averages. Also at night, the mean lower layer cloud heights are less than the means for water clouds in Table 5. It should be noted that the results in Table 5 are for all clouds and will include multilayered clouds that should cause the water cloud heights to be too high and the ice cloud heights to be too low. Additionally, there are some sampling population differences than can contribute to the differences.

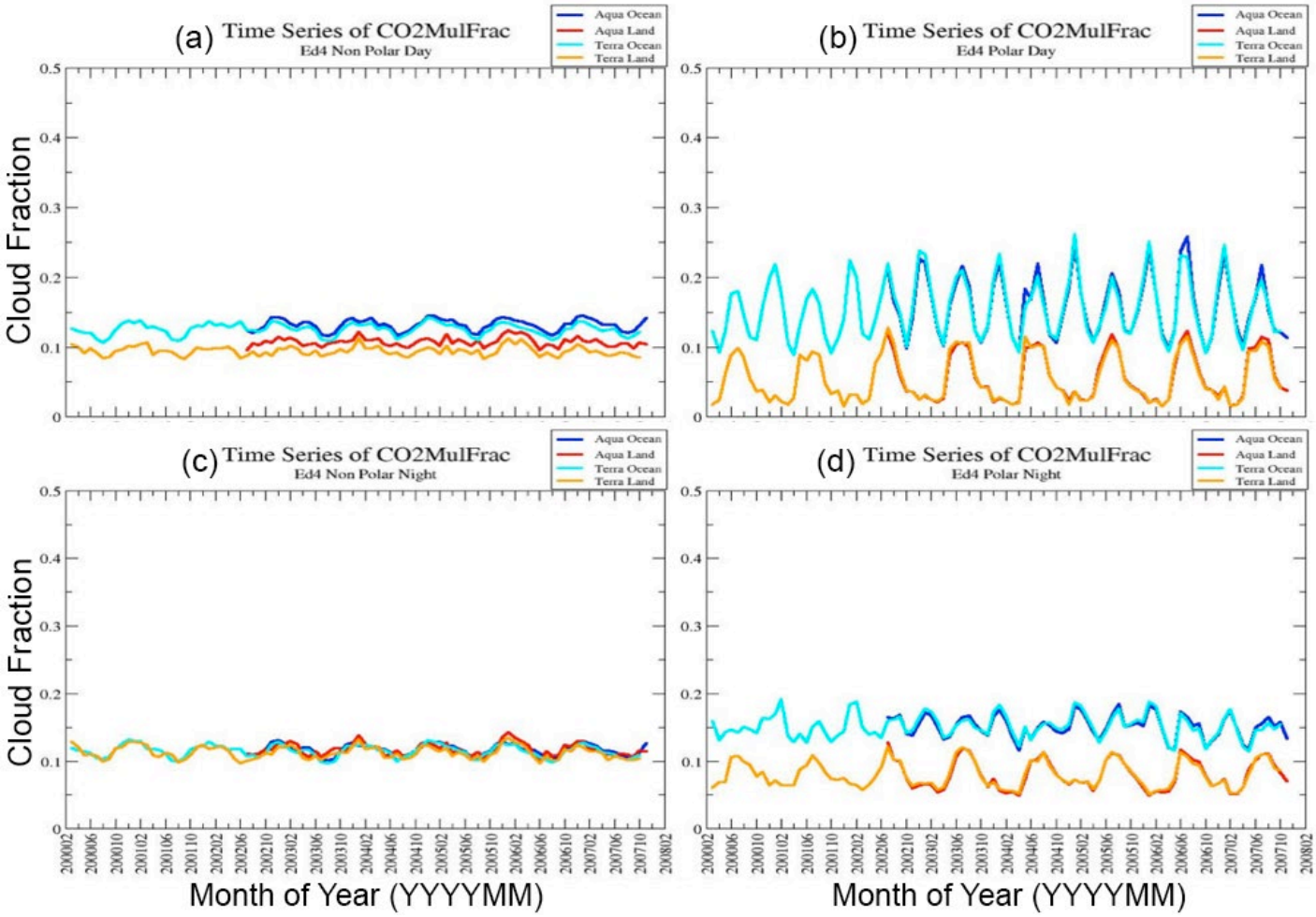

Figure 19. Same as Figure 17, except for multilayer cloud fraction.

Multilayer infrared optical depth, cloud effective water droplet and effective ice crystal radius are also retrieved for both lower and upper layers, respectively. Consistency between the Aqua and Terra is seen (not shown) for all of the parameters. The multilayer products can be considered experimental in Ed4 and are not expected to detect all multilayer clouds or to have no false detections. Rather, these products serve as an initial database for exploring the quality of the results, for initial studies of the impact of multilayer clouds on the radiation budget, and for development of more refined methods for multilayer cloud diagnosis and retrieval.

Table 10. Multilayer cloud fraction from Aqua Ed4 (2002-2007) and Terra Ed4 (2000-2007).

	Ocean			Land			Ocean & Land		
	Non-polar	Polar	Global	Non-polar	Polar	Global	Non-polar	Polar	Global
					Daytime				
Aqua	0.14	0.16	0.14	0.11	0.06	0.11	0.13	0.12	0.13
Terra	0.13	0.16	0.13	0.10	0.06	0.10	0.12	0.12	0.12
					Nighttime				
Aqua	0.12	0.16	0.13	0.12	0.09	0.12	0.12	0.12	0.12
Terra	0.12	0.16	0.12	0.12	0.09	0.11	0.12	0.12	0.12

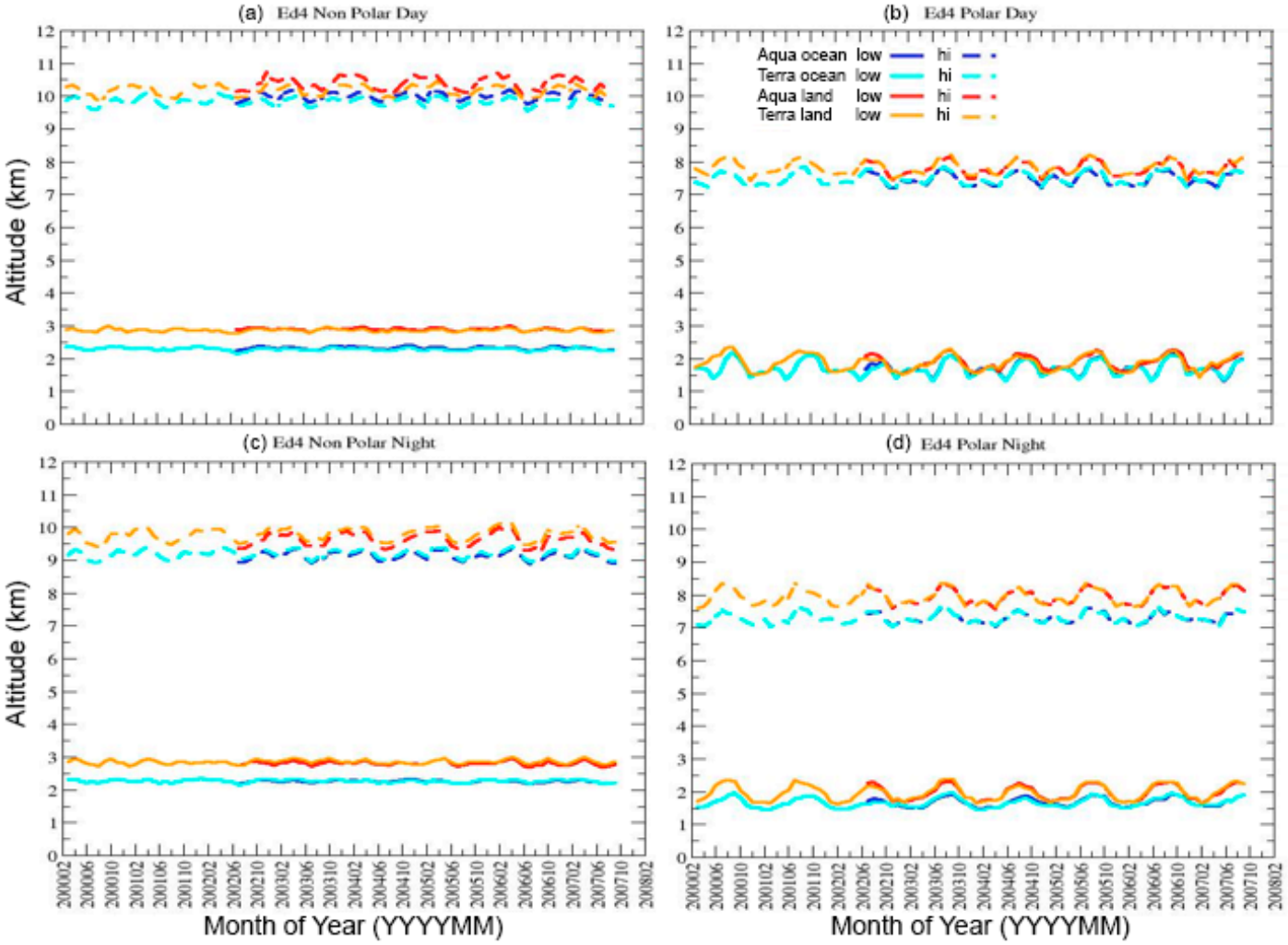

Figure 20. Same as Figure 17, except for multilayer cloud top height for upper and lower layers.

Given the results presented in this section, it is concluded that the CERES Ed4 Terra and Aqua cloud properties are consistent in all facets, at least for the time period available at the time of writing. They represent a significant improvement over the Ed2 analyses, which produced some distinct differences in the retrieved cloud properties that are not attributable to diurnal variability. Further trend studies including data taken after 2008 will be performed to ensure that this consistency continues and that the calibrations used in the Ed4 analysis remain reliable through the period of record.

Table 11. Multilayer cloud top height (km) for upper and lower layers. Aqua Ed4: 2002-2007; Terra Ed4: 2000-2007.

	Ocean			Land			Ocean & Land		
	Non-polar	Polar	Global	Non-polar	Polar	Global	Non-polar	Polar	Global
					Day				
Aqua (upper)	10.00	7.47	9.75	10.40	7.79	10.17	10.10	7.58	9.84
Terra (upper)	9.84	7.49	9.60	10.18	7.82	9.97	9.92	7.60	9.68
Aqua (lower)	2.33	1.71	2.27	2.90	1.87	2.81	2.48	1.77	2.41
Terra (lower)	2.30	1.71	2.25	2.88	1.88	2.79	2.45	1.78	2.39
					Night				
Aqua (upper)	9.14	7.31	8.91	9.63	7.94	9.44	9.25	7.58	9.03
Terra (upper)	9.19	7.30	8.96	9.78	7.95	9.57	9.33	7.58	9.10
Aqua (lower)	2.27	1.69	2.20	2.82	1.97	2.72	2.41	1.81	2.33
Terra (lower)	2.28	1.68	2.20	2.86	1.98	2.76	2.43	1.82	2.35

Comparison with other measurements

Cloud amount:

The primary changes to the cloud mask between Ed2 and Ed4 were implemented to improve cloud detection over polar regions and areas with thin cirrus and trade cumulus. Whereas the Ed2 Terra and Aqua masks had some slight differences, the same mask is used for both Terra and Aqua in Ed4. Aqua Ed4 data were compared to CALIPSO data for July 2013 to assess the accuracy of the cloud mask. The CALIPSO Vertical Feature Mask (VFM) was used to match the 5-km and 333-m cloud layers products with the nearest CERES MODIS pixel retrieval. Any MODIS pixels located within a 2.5-km radius from the center of the 5 km CALIPSO footprint are considered matches with CALIPSO, which typically yields one to two MODIS pixels. When multiple matching MODIS pixels are found, the mean of each MODIS cloud property is computed giving equal weight to each pixel. The MODIS and CALIPSO data were taken within a few minutes of each other. For CERES, a cloudy outcome is determined if CF $\geq$ 0.50. In practice, CF is usually equal to 0.0 or 1.0 because often only one MODIS pixel is matched to a given CALIPSO 5-km segment. For CALIPSO, a cloudy outcome is determined if the 5-km product reports one or more cloud layers or if the CF computed from the 0.33-km product exceeds 0.50. In addition, all CALIPSO cloud detections must be assigned a Quality Assurance (QA) Flag value of 3, indicating the highest confidence that the signal comes from a cloud and not clear air, aerosols, the surface, etc. All scenes containing any amount of cloud detected by CALIPSO at the 80-km scale are excluded from the analysis even if the QA Flag is set to 3. It is assumed that MODIS is unable to detect these very weakly scattering/absorbing clouds.

The results of the mask comparisons are summarized in Table 12. Overall, the Ed4 cloud mask agrees with CALIPSO 90% of the time, day and night, over all surfaces where snow or ice cover is absent. Agreement decreases over land, in general, because of larger uncertainties in the surface temperatures and reflectivities relative to ocean. Thus, the mask tends to underestimate clouds over land both day and night while being relatively unbiased over ice-free ocean. Over snow/ice-covered areas, the agreement decreases to 89% during the day and 77% at night. The latter number reflects the difficulty of distinguishing clouds from the extremely cold surfaces during the polar night. Cloud amounts over snow/ice surfaces are underestimated by 0.02 and 0.11, on average, during day and night, respectively. Overall, as shown in Table 3, the Ed4 mean global cloud fraction is 0.668, which represents an increase of ~0.06 relative to Ed2, bringing it much closer to the CALIPSO average. The Ed4 cloud fraction is clearly more accurate than that from the earlier edition.

Table 12. Comparison of CERES Ed4 cloud mask to matched CALIPSO data, July 2013.

Day	Fraction Correct	Bias	False Alarm Rate	Heidke Skill Score	Number of Matches
Nonpolar, Land, Snow/Ice-free	0.885	-0.063	0.046	0.76	301696
Polar, Land, Snow/Ice-free	0.887	-0.065	0.035	0.73	96599
Nonpolar, Ocean, Snow/Ice-free	0.905	-0.004	0.062	0.76	768434
Polar, Ocean, Snow/Ice-free	0.925	0.033	0.061	0.68	104171
Global, Land & Ocean, Snow/Ice-free	0.901	-0.020	0.057	0.76	1270897
Global, Land & Ocean, Snow/Ice-covered	0.887	-0.016	0.062	0.67	248077
Night					
Nonpolar, Land, Snow/Ice-free	0.873	-0.081	0.043	0.74	299213
Polar, Land, Snow/Ice-free	0.884	-0.034	0.060	0.73	64369
Nonpolar, Ocean, Snow/Ice-free	0.910	-0.024	0.042	0.72	846030
Polar, Ocean, Snow/Ice-free	0.943	-0.003	0.030	0.63	55303
Global, Land & Ocean, Snow/Ice-free	0.902	-0.037	0.043	0.73	1264915
Global, Land & Ocean, Snow/Ice-covered	0.765	-0.110	0.104	0.49	534546

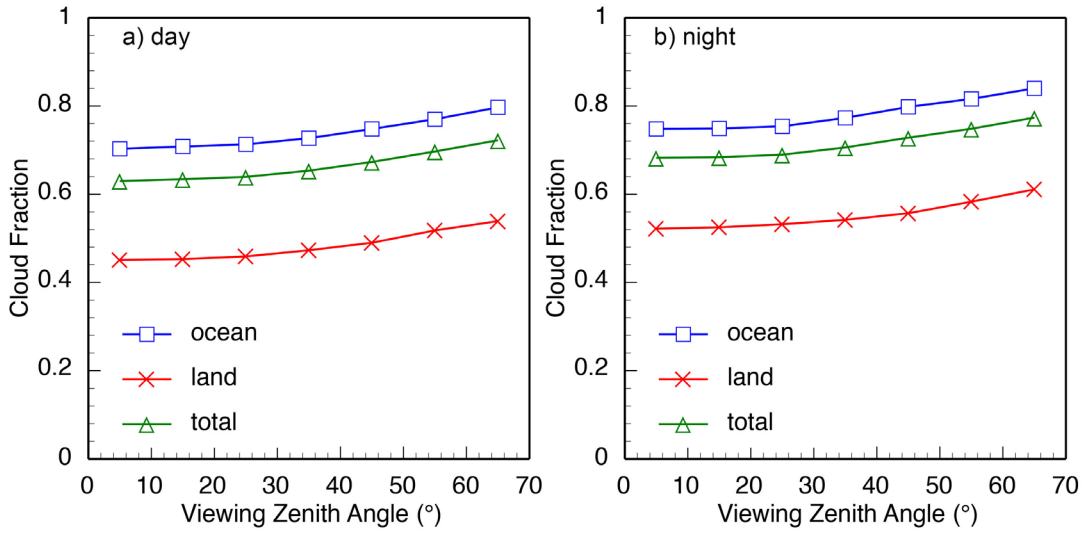

Figure 21. Mean 2004 global cloud fraction from Aqua CERES-MODIS mask as a function of viewing zenith angle.

Cloud detection tends to increase with viewing zenith angle (VZA) because the 3-D structure of clouds blocks broken clear areas, pixel resolution decreases (e.g., Minnis et al. 1989), and the path length of the scattering or emitting cloud particles rises as the view becomes more oblique. The CALIPSO comparisons used near-nadir observations and so do not represent the cloud mask overall. Figure 21 shows the VZA-dependence of mean cloud fraction from 2004 Aqua MODIS for day and night. During daytime (Figure 21a), the changes from 5° to 65° are 0.094, 0.088, and 0.092 for ocean, land, and all surfaces. The corresponding relative changes are 13, 19, and 15%. At night (Figure 21b), the respective absolute (relative) changes are 0.092 (12%), 0.089 (17%), and 0.091 (13%). Following the curves in Figure 21a, the average relative increase in cloud over the full VZA range of 70° is ~15%. The overall mean roughly corresponds to the cloud fraction at 40°.

Table 13. Same as Table 12, except for single-layer cloud phase.

Day	Fraction Correct	Ice FAR	Water FAR	Heidke Skill Score	% of matched cloudy pixels
Nonpolar, Land, Snow/Ice-free	0.951	0.010	0.106	0.897	33.8
Polar, Land, Snow/Ice-free	0.940	0.028	0.087	0.881	22.6
Nonpolar, Ocean, Snow/Ice-free	0.972	0.021	0.032	0.943	49.5
Polar, Ocean, Snow/Ice-free	0.957	0.052	0.041	0.857	27.9
Global, Land & Ocean, Snow/Ice-free	0.967	0.020	0.043	0.932	42.9
Global, Land & Ocean, Snow/Ice-covered	0.926	0.113	0.063	0.795	23.0
Nighttime					
Nonpolar, Land, Snow/Ice-free	0.908	0.043	0.210	0.772	35.3
Polar, Land, Snow/Ice-free	0.868	0.116	0.153	0.731	27.8
Nonpolar, Ocean, Snow/Ice-free	0.952	0.067	0.034	0.901	42.3
Polar, Ocean, Snow/Ice-free	0.885	0.200	0.034	0.769	35.3
Global, Land & Ocean, Snow/Ice-free	0.939	0.070	0.052	0.878	37.3
Global, Land & Ocean, Snow/Ice-covered	0.876	0.132	0.064	0.539	43.6

Cloud phase:

Cloud phase was validated by comparing the phase selections from Ed4 to those from CALIPSO (Hu et al. 2009) using only single-phase clouds for MODIS pixels having CALIPSO cloud fractions of 100%. That is, cloud matches having a single phase throughout the CALIPSO column regardless of the number of distinct layers were used to verify the cloud phase and for the cloud height comparisons in the next section. The analyzed cases represent about 45% of the matching cloudy pixels over snow/ice-free areas and ~36% over snow/ice-covered areas. The results in Table 12 reveal ~97% and 94% agreement over snow/ice-free regions during day and night, respectively. Over snow/ice covered areas, ~91 and 88% congruity is seen during day and night, respectively. The phase determination over land is slightly less accurate than over ocean during daytime compared to CALIPSO. At night the land-ocean phase agreement difference increases. Combining the snow/ice-free and -covered results, weighting by the total number of single-layer clouds used in the comparisons, yields 96.1 and 92.1% agreement globally, regardless of underlying surface type, during day and night, respectively.

Because the standard Ed4 retrievals assume that each pixel contains only a single-layer, single-phase cloud, the Ed4 phase selection for multi-layer or mixed phase clouds depends on the thickness of the upper-layer ice clouds relative to that of the underlying water clouds. This dependence was examined by comparing with October 2008 CALIPSO data in which non-opaque ice clouds co-occurred with lower-level water clouds (no limit on thickness) and both the ice and water layers covered 100% of the 5-km footprint (Figure 22). During daytime in these cases (Figure 22a), 99% of the upper-layer ice clouds had a CALIPSO cumulative optical depth, $\tau_{ice} < 1.33$ and 50% had $\tau_{ice} < 0.066$. Only 10% of the cases had $\tau_{ice} > 0.62$. At night (Figure 22b), 99% of the cases had $\tau_{ice} < 1.64$ and 50% had $\tau_{ice} < 0.054$. Only 10% of the cases had $\tau_{ice} > 0.55$. Most of the ice clouds had $\tau_{ice} < 0.1$. Figure 22c and Figure 22d show the phase selection as a function of τ_{ice} for day and night, respectively. A very small fraction of the ML cloud cases were missed entirely by the Ed4 mask for $\tau_{ice} < 0.2$, presumably for those cases when the lower cloud optical depth was also very small. During the day (Figure 22c), the phase is more likely to be ice if $\tau_{ice} > 0.57$. At night (Figure 22d), this 50% threshold drops to 0.37. Given the relative populations of τ_{ice} probabilities in the upper half of Figure 22, ~80% of the ML clouds, as defined here, will be classified as water during the daytime, at least at near-nadir view angles. At night, ~65% of the ML clouds will be classified as liquid water clouds when $\tau_{ice} < 1.5$. It is expected that when $\tau_{ice} > 1.5$, the phase accuracy should be similar to that for single layer clouds. Because the ice cloud path length increases with VZA, it is expected that a greater percent of the ML clouds will be classified as ice at higher VZAs. This VZA dependence can only be tested using passive retrievals from an imager that is out of the A-Train.

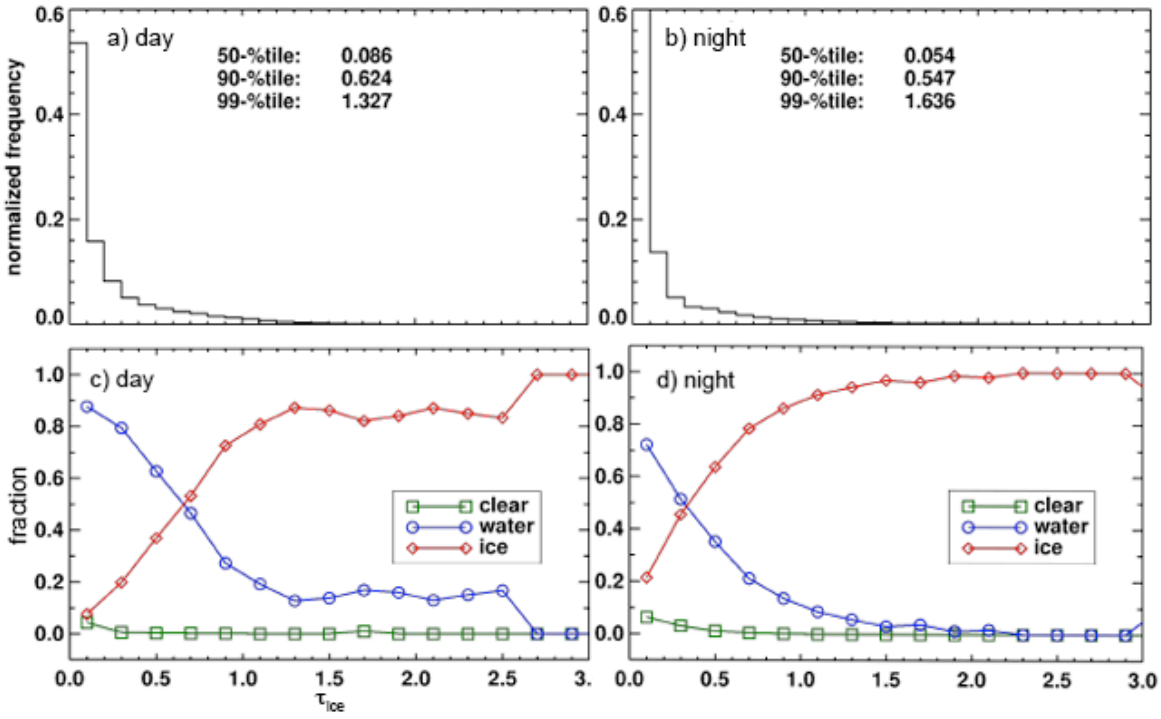

Figure 22. Mean 2004 global cloud fraction from Aqua CERES-MODIS mask as a function of viewing zenith angle.

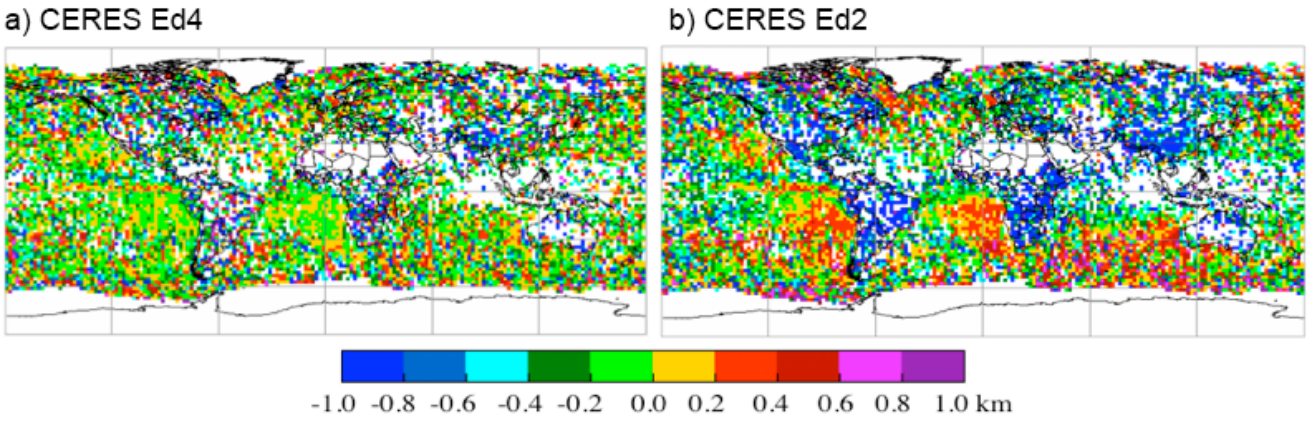

Figure 23. Regional mean daytime low-cloud top height differences, MODIS – CALIPSO, for CERES MODIS retrievals for October 2007 using matched pixel data having CALIPSO cloud tops below 4 km. From *Sun-Mack at el.* (2014).

Cloud height, pressure, and temperature:

These parameters are all related because the cloud temperature is used to ascertain cloud height and the height is used to select the pressure. For Ed4, cloud effective height, temperature, and pressure are reported together with cloud top height, temperature, and pressure, and cloud base height, temperature, and pressure. Only cloud top height is compared with the CALIPSO data for liquid clouds, since it is the only directly comparable quantity and the difference between Z_e and Z_t is minimal. The effective and cloud top heights are significantly different for ice clouds and effective cloud is included in the comparisons with CALIPSO to quantify the differences. The comparisons are performed separately for opaque and non-opaque clouds, where opaque refers to the absence of a return lidar signal from the surface. It typically occurs for clouds having an optical depth > 2 or so.

To validate the lapse rate method described above, Sun-Mack et al. (2014) compared retrieved low cloud heights with CALIPSO for two months using fully sampled (all available pixels used) MODIS data. The results used only single-layer, water-phase clouds having a cloud-top height below 4 km according to CALIPSO. They also showed how the Ed4 algorithm performed relative to several other techniques. Figure 23 shows a subset of those results, the average differences between the CERES-MODIS Ed4 and Ed2 retrievals and CALIPSO for those single-layer liquid clouds having CALIPSO heights below 4 km for October 2007. The agreement between CALIPSO and Ed4 is better and the distribution of the differences more random than they are for the Ed2 results.

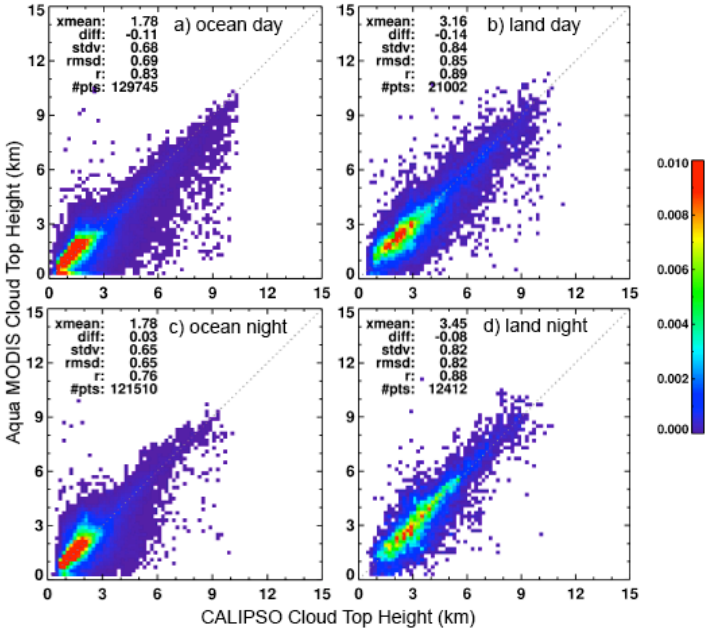

Figure 24. Scatterplots and statistics of opaque, SL cloud top heights from matched CERES Ed4 Aqua MODIS and CALIPSO retrievals, July 2013. Color bar indicates fraction of total number of samples in a given 0.2 km x 0.2 km bin.

Table 14. Differences between Aqua Ed4 and CALIPSO cloud top heights for all non-opaque and opaque single-layered, liquid clouds, July 2013. Biases are computed as Aqua – CALIPSO.

	Non-Opaque			Opaque		
Day	**Bias (SDD) [km]**	**R**	**Number of Matches**	**Bias (SDD) [km]**	**R**	**Number of Matches**
Global, Ocean, Snow/Ice-free	-0.02 (0.67)	0.74	43673	-0.11 (0.68)	0.83	129745
Global, Land, Snow/Ice-free	-0.26 (1.13)	0.72	5762	-0.14 (0.84)	0.89	21002
Global, Land & Ocean, Snow/Ice-covered	-0.04 (0.83)	0.71	9142	-0.53 (0.91)	0.83	21047
Night						
Global, Ocean, Snow/Ice-free	0.08 (0.58)	0.78	40654	0.03 (0.65)	0.76	121510
Global, Land, Snow/Ice-free	0.07 (0.85)	0.79	4499	-0.08 (0.82)	0.87	12412
Global, Land & Ocean, Snow/Ice-covered	0.38 (0.84)	0.44	3550	0.28 (0.91)	0.59	8146

To further validate the water cloud heights, the operational subsampled Ed4 results are compared with CALIPSO data from July 2013. The water cloud comparisons utilize all single-phase liquid water clouds with no height restriction on the CALIPSO data. Figure 24 presents the scatterplots for opaque SL water clouds over snow-free areas. For the most part, the data are centered about the lines of agreement. A slight discontinuity is evident in the ocean plots (Figure 24a, c) around 2.2 km, which roughly corresponds to the pressure height where the lapse rate starts transitioning to the model sounding. No discontinuity is apparent in the land plots (Figure 24b, d). The statistics listed in each plot indicate the quality and level of agreement for each case.

The results were lumped into three categories: snow/ice-free ocean and land, and snow/ice-covered. The last category includes both ocean and land surfaces. Table 13 lists the biases and standard deviations of the differences (SDD) for non-opaque and opaque clouds during July 2013. During daytime, the magnitudes of the opaque biases are slightly larger the non-opaque values, while the opposite occurs for nighttime. The non-opaque SDDs tend to be somewhat greater than their opaque counterparts, except over the cryosphere. Larger uncertainties are expected for non-opaque clouds because the height is dependent on the optical depth and observed temperature. The correlation coefficients, *R*, reflect these increased uncertainties, being greater for the opaque clouds, both day and night.

Table 14 combines the opaque and non-opaque results from Table 13 for comparison with the October 2007 and January 2009 results from Sun-Mack et al. (2014) for all SL clouds, opaque and non-opaque, for which the CALIPSO cloud top height was < 4 km. Overall during daytime, the magnitudes of the biases tend be larger than found by Sun-Mack et al. (2014), however, the SDD values are comparable for all 3 months. The biases are worst over snow/ice surfaces. Some of the bias may be due to the pressure limits used to apply the lapse rate method. Decreasing the value of transition pressure to 700 hPA could reduce the average bias.

Table 15. Same as Table 13, except for all SL water clouds during July 2013. Values in two rightmost columns from Sun-Mack et al. (2014) for all liquid clouds with CALIPSO heights below 4 km.

	July 2013	**October 2007**	**January 2009**
Day	**Bias (SDD) [km]**	**Bias (SDD) [km]**	**Bias (SDD) [km]**
Global, Ocean, Snow/Ice-free	-0.09 (0.68)	0.04 (0.61)	0.02 (0.67)
Global, Land, Snow/Ice-free	-0.17 (0.91)	-0.06 (0.85)	-0.08 (0.95)
Global, Land & Ocean, Snow/Ice-covered	-0.38 (0.91)	0.38 (0.95)	-0.17 (0.91)
Night			
Global, Ocean, Snow/Ice-free	0.04 (0.66)	0.10 (0.62)	0.10 (0.68)
Global, Land, Snow/Ice-free	-0.04 (0.84)	-0.01 (0.83)	-0.02 (0.88)
Global, Land & Ocean, Snow/Ice-covered	0.31 (0.89)	0.03 (0.92)	-0.17 (0.95)

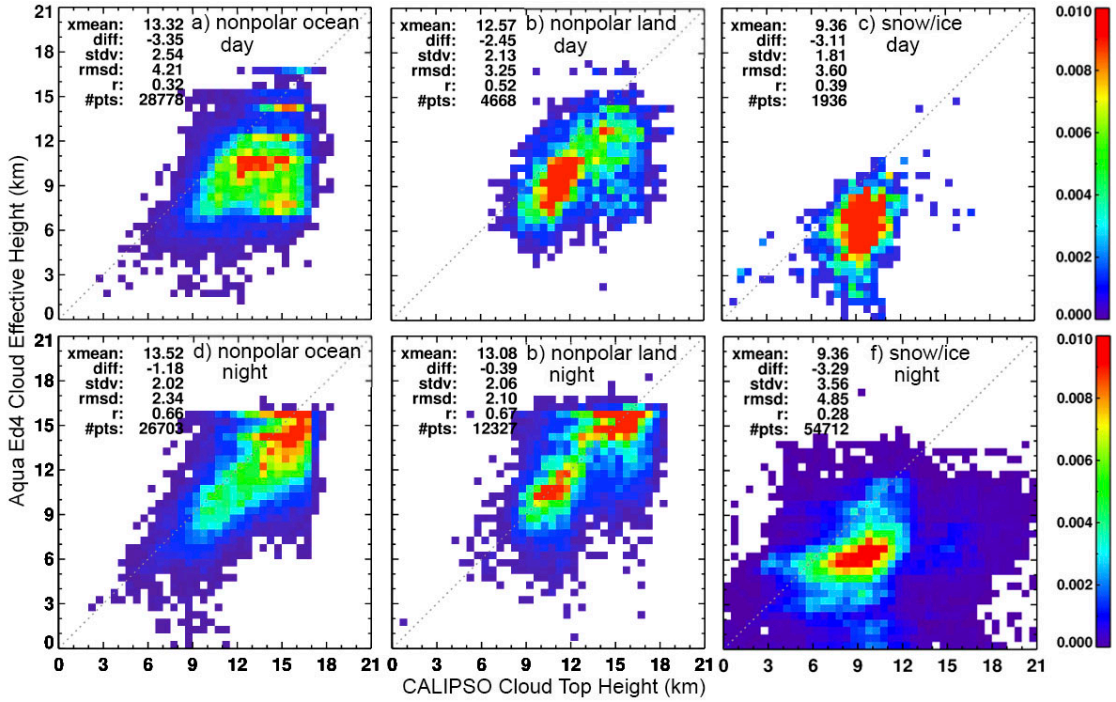

Figure 25. Comparisons of SL non-opaque ice cloud effective height between Aqua Ed4 and CALIPSO, July 2013. Color bar indicates fraction of total number of samples in a given 0.5 km x 0.5 km bin.

Similarly, SL ice cloud effective (Figure 25) and top (Figure 26) heights were compared with CALIPSO data for both July 2013 and for October 2008. Over nonpolar areas, the absolute biases and SDDs are generally smaller at night (Figure 25d, e; Figure 26d, e) than during the day (Figure 25a, b; Figure 26a, b). The exception is for data taken over snow and ice. The parameterizations used to convert cirrus Z_e to Z_t (Minnis et al. 2011) reduce the absolute bias during the day by 1.2 to 1.5 km depending on the surface. At night, the range is 0.2 km over land to 1.8 km over ocean. The day-night difference in bias change is due to two factors. The larger optical depths during the day (see below) yield larger values of T_e, which in turn, returns a greater height correction from the parameterizations. Additionally, the correction is constrained so that Z_t does not exceed the tropopause height. At night, the correction likely hits this limit more frequently because the values of Z_e are typically greater than those during daytime. Over snow/ice surfaces, both the bias and SDD are much worse day and night because of larger uncertainties in the surface temperatures over the cryosphere. The smaller nocturnal biases are due to the use of IR channels alone to determine τ, which is used in the correction to obtain the effective cloud temperature. During the day, the new ice crystal models are not sufficient to yield the required smaller infrared optical depths (see optical depth comparisons in the next section). The greatest errors in nonpolar regions are found for the highest cirrus clouds, which likely have the smallest values of τ. At night, the correlation coefficients over nonpolar areas are comparable to their low cloud counterparts. During daytime, the Aqua height retrievals over land seem to be in much better agreement than over nonpolar ocean.

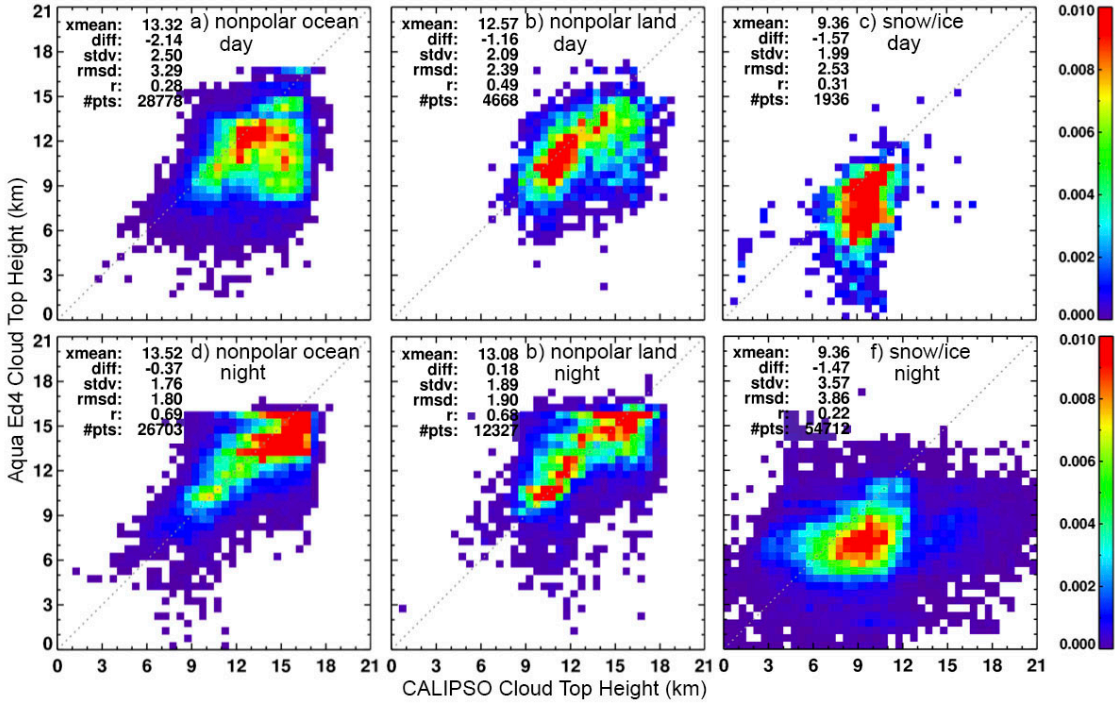

Figure 26. Comparisons of SL non-opaque ice cloud top height between Aqua Ed4 and CALIPSO, July 2013. Color bar indicates fraction of total number of samples in a given 0.5 km x 0.5 km bin.

Table 16. Differences, Aqua Ed4 – CALIPSO, cloud top heights for single-layered, non-opaque ice clouds.

	Bias [km]		SDD [km]		Number of Matches
	Non-opaque defined by CALIPSO, July 2013 and October 2008				
Day	**top**	**effective**	**top**	**effective**	
Global, Ocean, Snow/Ice-free	-2.23	-3.36	2.77	2.79	66018
Global, Land, Snow/Ice-free	-1.33	-2.62	2.37	2.32	16575
Global, Snow/Ice-covered	-1.77	-3.56	2.99	3.05	31373
Night					
Global, Ocean, Snow/Ice-free	-0.23	-1.07	1.91	2.17	56344
Global, Land, Snow/Ice-free	-0.23	-0.84	2.18	2.46	34202
Global, Snow/Ice-covered	-1.49	-3.06	3.20	3.36	54712
	Non-opaque defined as $\tau < 6$, October 2008				
Day	**top**	**effective**	**top**	**effective**	
Global, Ocean, Snow/Ice-free	-1.99	-3.12	2.66	2.68	59188
Global, Land, Snow/Ice-free	-1.43	-2.59	2.29	2.37	18935
Global, Snow/Ice-covered	-3.11	-4.06	2.37	2.57	16436
Night					
Global, Ocean, Snow/Ice-free	-0.53	-1.53	1.90	2.08	73094
Global, Land, Snow/Ice-free	-0.59	-1.39	2.00	2.24	38949
Global, Snow/Ice-covered	-1.57	-2.22	2.08	2.26	51828

Table 15 further summarizes the non-opaque ice cloud (NOC) height differences using the same categories employed for the water cloud analyses and including data both October 2008 and July 2013. The effective height absolute biases are substantially greater than those for Z_t, as expected. The SDD values are roughly 2-3 times their water cloud counterparts. The nearly equivalent day-night biases and larger nocturnal SDD over ice/snow surfaces indicate the need for a reevaluation of the approaches used to determine thin-cloud optical depths over the cryosphere. Also included in Table 15, is a summary of the differences for October 2008 results non-opaque clouds defined, not on the basis of CALIPSO receiving a return from the surface, but on the optical depth retrieved by the MODIS retrieval algorithm. In this case, it is assumed that $\tau < 6$ indicates a NOC. This approach is used because it is helpful to understand the errors in terms of the retrieved optical depths, since the user has no knowledge of the CALIPSO opacity. Although not shown, the use of $\tau < 6$ as an opaque threshold yields significantly more NOCs both day and night over non-polar regions but fewer non-opaque clouds during the day over snow/ice areas. The results over nonpolar areas are smaller biases and SDDs for $\tau < 6$ during daytime, but greater biases and smaller SDDs at night. Over the snow/ice surfaces, Z_t is less biased with smaller SDDs for $\tau < 6$.

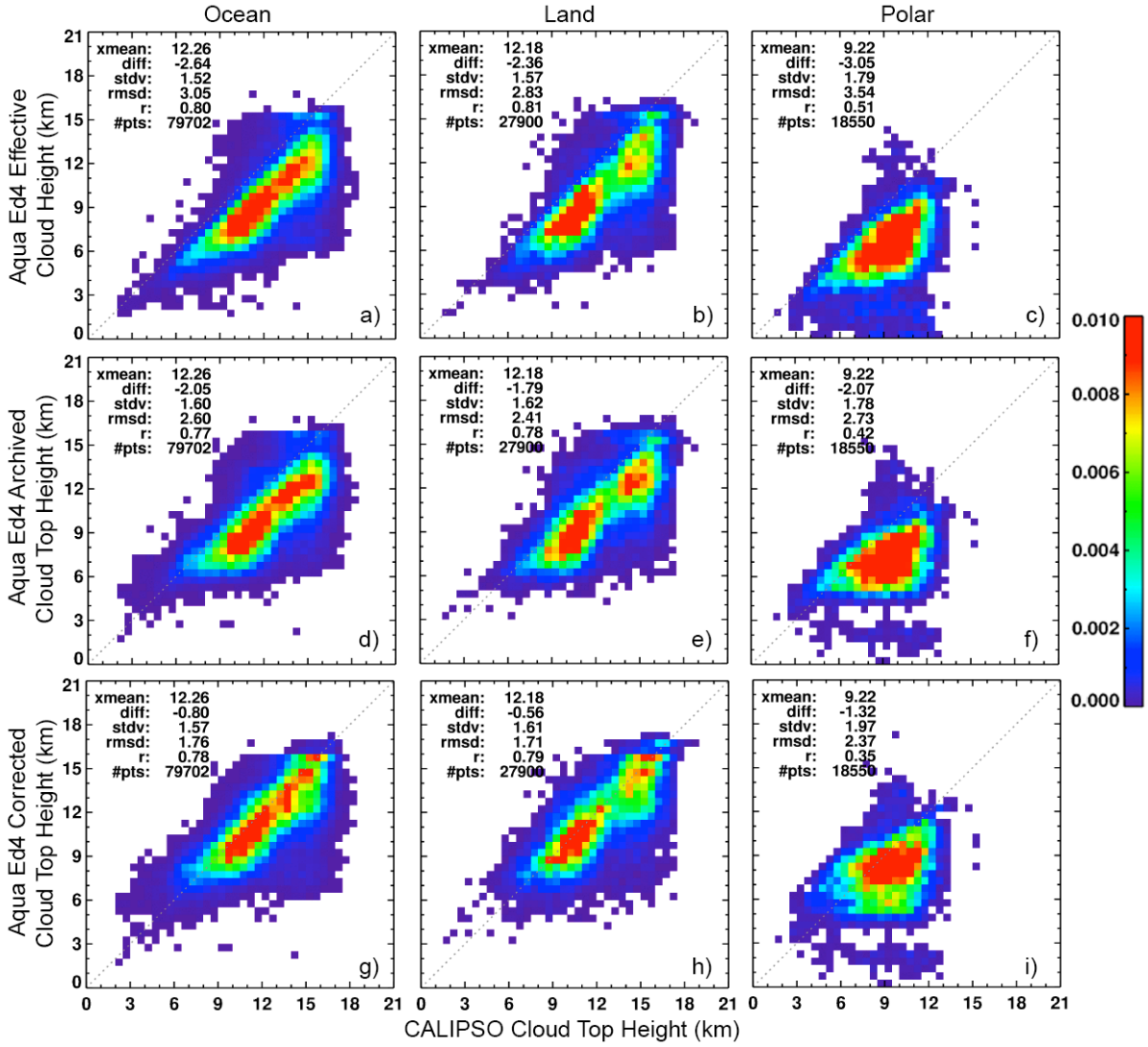

Figure 27. Comparisons of opaque ice cloud effective (a, b, c) and top heights between Aqua Ed4 and CALIPSO, daytime October 20008. (d, e, f) archived cloud-top height values. (g, h, i) archived values with correction (Eq. 2) applied *ex post facto*.

The October 2008 daytime opaque ice cloud (OC) heights are compared with CALIPSO cloud-top heights in Figure 27 for Z_e (top), the archived Z_t values (middle), and the archived Z_t data corrected *ex post facto* with Eq (2) (bottom). The effective heights have the largest biases, as expected, but show the greatest correlation coefficients and smallest SDD values. Over non-polar regions, the effective height absolute biases (Figure 27a, b) are roughly 0.5 km greater than the archived cloud-top heights (Figure 27d, e). In polar areas, the archived top height absolute biases (Figure 27f) are ~1 km less than the effective heights (Figure 27c), which underestimate the cloud tops by 3 km. Application of Eq (2) decreases the absolute bias by more than 1.2 km over the nonpolar regions (Figure 27g, h) and by ~0.7 km over the polar regions (Figure 27i) relative to the archived Z_t.

The OC height differences for day and night are summarized in Table 16 for the same categories used in Table 15. The absolute biases in Z_e are smaller at night. While the magnitudes of the Z_t biases for the nocturnal archived data are about 0.6 km smaller than those during daytime, the *ex post facto* corrections to the nighttime data yield roughly the same biases and SDDs over snow/ice-free areas as in the daytime. The night corrections are 0.5 km less than the day values over cryospheric surfaces. Some of the diminished correction may be due to missing the threshold of $\tau = 6$ needed to apply the corrections. At night, the determination of τ is less certain than during the day, but the detection of an essentially black (in the infrared) cloud is relatively certain. During the day, an ice cloud having $\tau = 2$ or 3 might appear opaque to CALIPSO and thus could overlap a thick low cloud giving a total $\tau > 6$ according to

Table 17. Global cloud height differences in km, Aqua Ed4 heights – CALIPSO cloud top heights for opaque ice clouds.

	Effective			Top, Archived			Top, Corrected *ex post facto*			
	opaque defined by CALIPSO, July 2013 and October 2008									
Day	**Bias**	**SDD**	**R**	**Bias**	**SDD**	**R**	**Bias**	**SDD**	**R**	**Number**
Ocean, Snow/Ice-free	-2.66	1.48	0.82	-2.04	1.56	0.80	-0.84	1.58	0.80	168459
Land, Snow/Ice-free	-2.33	1.49	0.82	-1.78	1.54	0.80	-0.53	1.58	0.79	64626
Snow/Ice-covered	-2.79	1.64	0.54	-1.82	1.76	0.43	-1.01	1.87	0.36	24929
Night										
Ocean, Snow/Ice-free	-2.09	1.53	0.84	-1.31	1.53	0.82	-0.48	1.55	0.83	160615
Land, Snow/Ice-free	-2.00	1.65	0.79	-1.22	1.76	0.78	-0.61	1.70	0.80	59420
Snow/Ice-covered	-2.40	1.94	0.58	-1.67	1.82	0.60	-1.45	1.89	0.58	75255
	Opaque defined as $\tau \geq 6$, October 2008									
Day	**Bias**	**SDD**	**R**	**Bias**	**SDD**	**R**	**Bias**	**SDD**	**R**	**Number**
Ocean, Snow/Ice-free	-2.63	1.26	0.87	-2.23	1.41	0.84	-0.56	1.33	0.86	64251
Land, Snow/Ice-free	-2.38	1.38	0.87	-1.98	1.43	0.85	-0.35	1.38	0.86	24228
Snow/Ice-covered	-3.00	2.67	0.17	-1.22	2.53	0.10	0.11	2.57	0.15	30489
Night										
Ocean, Snow/Ice-free	-2.10	1.21	0.90	-1.66	1.26	0.90	-0.13	1.12	0.92	36285
Land, Snow/Ice-free	-2.47	1.69	0.85	-1.89	1.65	0.84	-0.42	1.62	0.85	12203
Snow/Ice-covered	-3.22	3.17	0.14	-1.25	2.79	0.15	-0.02	2.86	0.18	25285

the MODIS retrieval. In this case, no correction would be applied to account for the semitransparency of the upper-level cloud and Z_e would be underestimated, leading to the larger uncorrected average biases during the day relative to those at night. Adjustments for these shortcomings will be made in future editions. For OCs, the expected biases in Z_t after correction are roughly -0.6 ± 1.6 km and -1.2 ± 2.0 km over snow-free and snow-covered areas, respectively.

As in Table 15, Table 16 includes the results based on defining an opaque cloud (OC) using $\tau \geq 6$ as the threshold for determing an OC for October 2008. As exepected, fewer OCs are determined for the nonpolar areas and more for the polar regions during the day (not shown). At night, fewer OCs are found with $\tau \geq 6$ for all surfaces. The biases and SDDs are generally smaller for the $\tau \geq 6$ cases during both day and night, ostensibly due to the smaller dataset, which includes thicker clouds on average since CALIPSO becomes opaque at τ around 2 or 3. In any case, combining the OCs and NOCs together for both cases yields the same averages, as expected.

To examine the overall agreement with CALIPSO, the matched data were screened to include all cases having cloud fractions > 99% for both the CALIPSO footprints and MODIS pixels in each set of matched data. For CALIPSO clouds having more than one layer, the height of upper layer was assumed to represent the cloud top heights for CALIPSO. Figure 28 shows the July 2013 height difference histograms for all clouds and for SL clouds separately over nonpolar and polar areas. Overall, the Aqua MODIS Z_t measn are 1.8 and 1.3 km less than the highest CALIPSO cloud-top height (Figure 28a, c) for nonpolar and polar areas, respectively. The corresponding SDDs are 3.5 and 2.8 km, resulting from the large negative skew in the distribution (solid black). For clouds below 5 km (blue curve), there is essentially no bias, on average, with well-balanced differences and SDD = 1.0 km for nonpolar and 1.7 km for polar regions. For cloud tops above 5 km (red curve), the negative skew is more prominent resulting in a bias of -2.9 ± 4.0 km and -2.2 ± 3.0 km over nonpolar and polar regions, resepectively. The smaller polar SDD is likely the result of having a lower tropopause than in the tropics and not to any improved algorithmic accuracy. If only SL clouds are considered (Figure 28b, d), the biases and SDD drop dramatically, except for low cloud biases, which are 0.08 ± 0.75 km and 0.36 ± 1.6 km over nonpolar and polar areas, respectively.

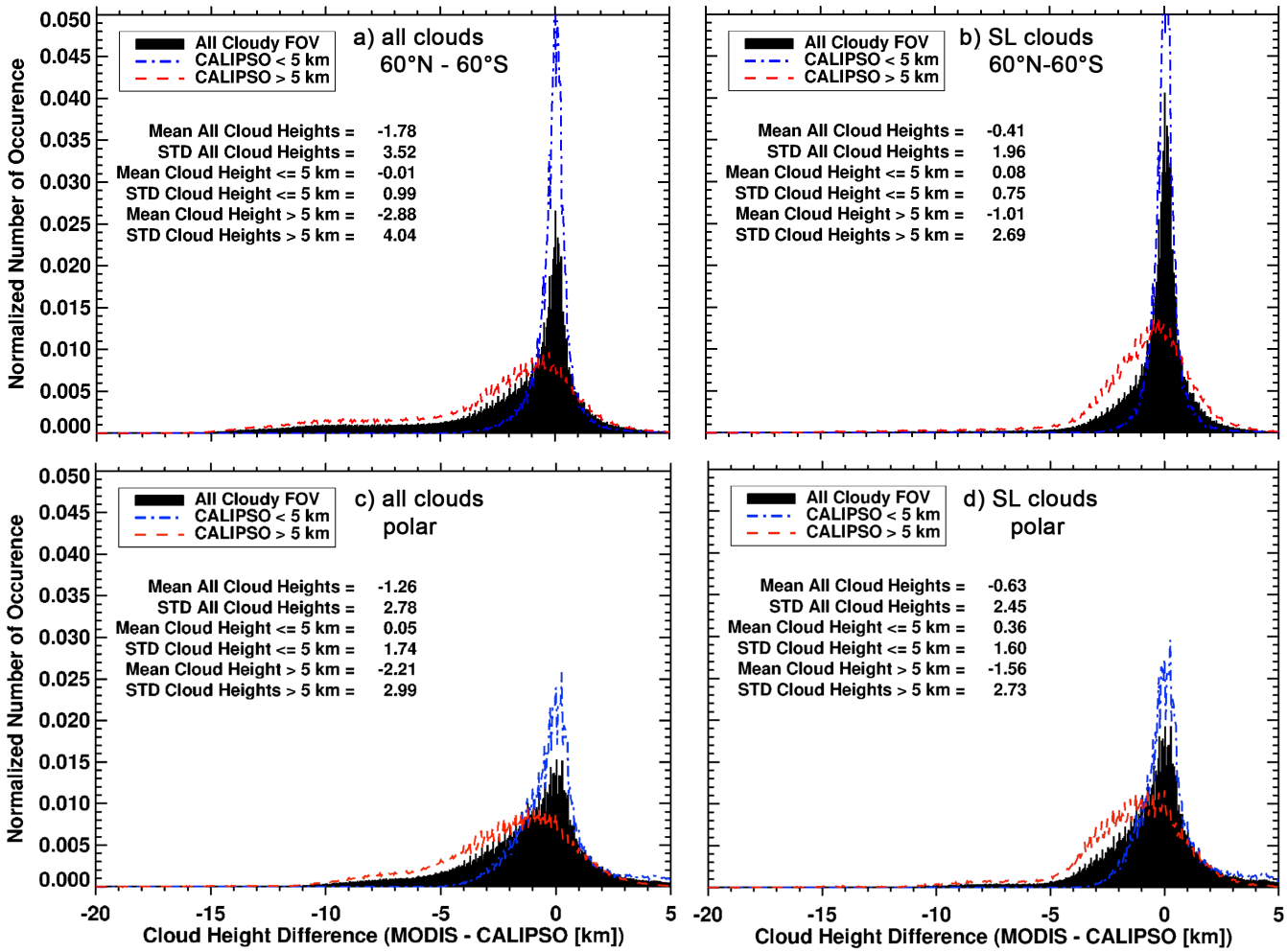

Figure 28. Cloud height difference histograms, Aqua MODIS – CALIPSO, for overcast matched footprints, July 2013, combined day and night.

In an independent study, Xi et al. (2014) compared SL stratus cloud-top and base heights determined from a cloud radar at Graciosa Island, Azores with matched Terra and Aqua Ed4 heights. The cloud base and height differences are 0.06 ±0.25 km and -0.07 ±0.28 km, respectively, during the daytime. At night, the corresponding differences are 0.14 ±0.34 and -0.04 and ±0.37 km. The mean cloud-top height biases are similar to those seen in the CALIPSO comparisons (Table 13), while base height differences are the first seen for the Ed4. The SDDs are surprisingly small, less than half those seen in the CALIPSO comparisons. Additional comparisons with other sources are needed to provide a more comprehensive assessment of the retrieved cloud base heights.

Since the standard retrieval assumes each pixel contains a SL cloud, the retrieved cloud temperature or height likely corresponds to a value somewhere between the upper and lower cloud levels. Using the matched CALIPSO-MODIS ML data set used for Figure 22, the difference between the MODIS-retrieved effective height and the average of the upper and lower layer top heights was computed for each ML pixel. Figure 29 plots the histograms of the differences (Z_t-CALIPSO mean height) as functions of τ_{ice}. As expected, the difference is most negative for $\tau_{ice} < 0.2$ and gradually becomes positive when τ_{ice} exceeds ~0.6 or so during the day (Figure 29a) and is greater than ~0.4 at night (Figure 29b). It is clear from the number of points (Figure 22a, b) that most of the cloud heights will be lower than the average of the low and high clouds, and will likely be classified as liquid water (e.g., Figure 22c, d). The distribution of the differences will likely change with VZA because of the increased path length of the upper layer cloud.

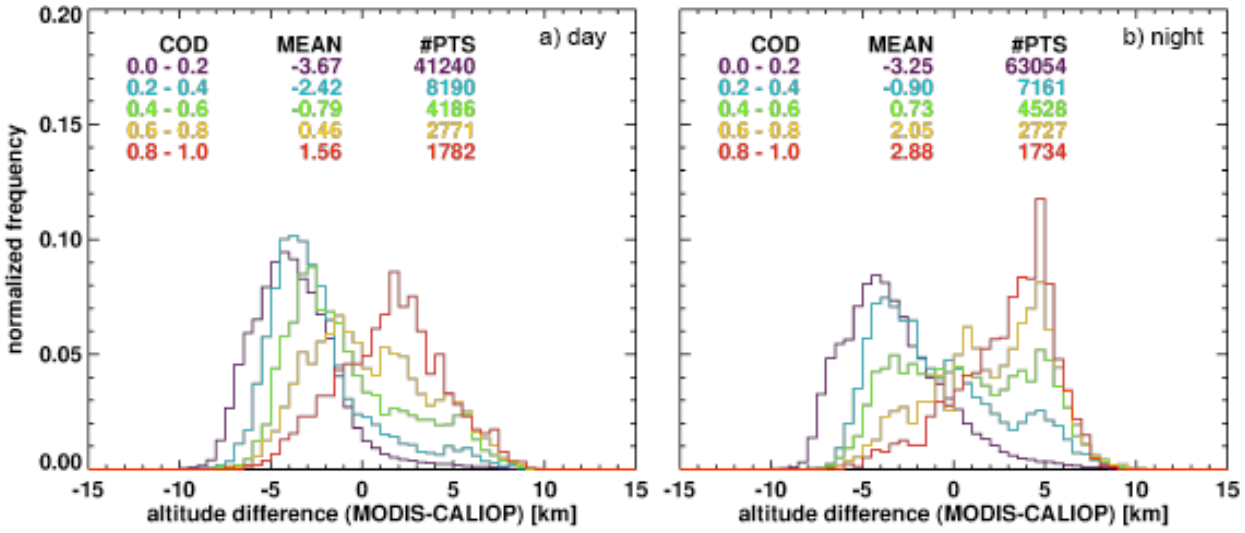

Figure 29. Mean 2004 global difference between Aqua CERES-MODIS cloud effective height and average of upper and lower-layer cloud –top heights from CALIPSO.

Cloud effective height can vary with VZA for several reasons, which include the increase in path length with VZA and 3-D effects. The former tends to raise the radiating layer (e.g., Minnis et al. 2008c), while the latter blocks contamination of partly cloudy pixels by clear portions of the pixel as the cloud amount rises with VZA. Similarly, lower cloud tops in heterogeneous clouds will tend to be blocked by higher cloud tops at large VZAs. Again, the matched CALIPSO comparisons used near-nadir observations and so do not represent the cloud mask overall. Figure 30 examines the global average VZA dependence of cloud effective height using the daytime Aqua results from 2004. For liquid water clouds (Figure 30a), Z_c increases between 5° and 65° by 0.129, 0.386, and 0.203 km for ocean, land, and all surfaces, respectively. For ice clouds (Figure 30b) over the same surfaces, Z_c increases by 0.554, 0.826, and 0.633 km, respectively. The overall mean Z_c corresponds to VZA = 40°, which for liquid clouds over ocean is nearly the same value as the nadir mean. Over land, the mean value is ~0.213 km higher than the nadir value, which suggests that considering all VZAs, on average, the liquid water cloud heights over land are probably less biased than the average of 0.200 km indicated in Table 13. For ice clouds, the mean Z_c at VZA = 40° is ~0.3 km greater than at 0°, and the mean ice cloud height biases in Table 15 and Table 16 and Figure 30 are probably smaller when measurements from all VZAs are considered.

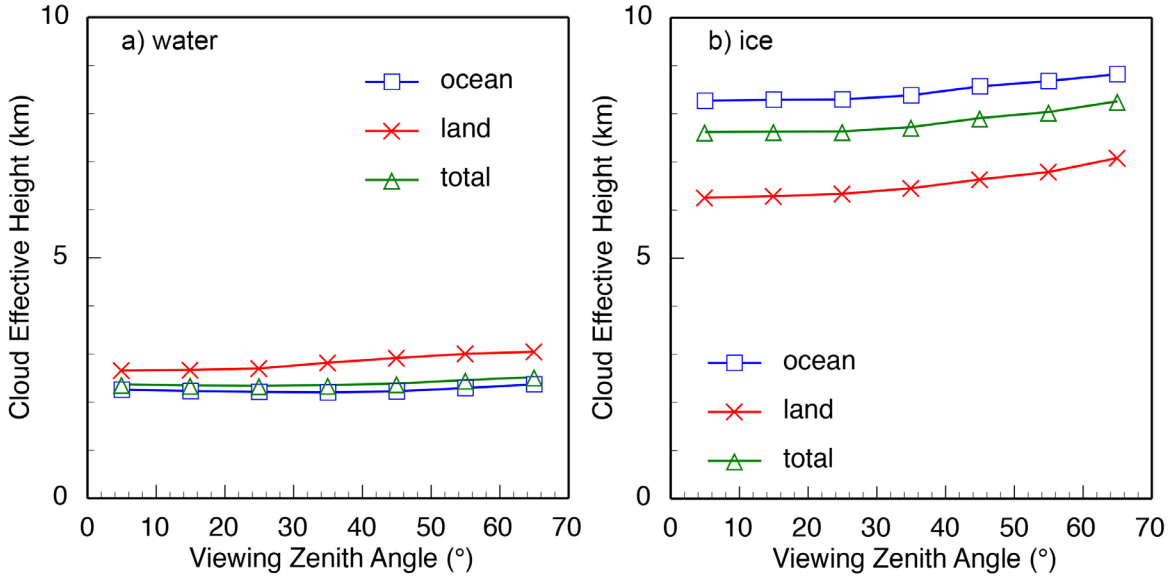

Figure 30. Mean 2004 global cloud effective height from Aqua CERES-MODIS mask as a function of viewing zenith angle.

Cloud optical depth, effective particle size, and water path

Cloud optical depth, particle effective radius, and water path from Ed4 were evaluated against Ed2 in the time series for both Terra and Aqua, shown in Figure 12 (optical depth) and Figure 14 (particle size in radius) for water clouds and Figure 13 and Figure 15 for their ice cloud counterparts. Table 6, Table 7, and Table 8, which quantify the averages in τ, r_e, and *WP*, reveal that over ocean the water cloud mean τ increased by 6 and 75% over nonpolar and polar areas, respectively, relative to Ed2. The corresponding ice cloud mean optical depths dropped by 1.5% over nonpolar (NP) regions and and rose by 63% over the poles. Water cloud mean effective radius increased by 4% (0.5 µm) over NP areas and remained essentially unchanged over polar regions. For ice clouds, r_e dropped by 2% (0.6 µm) in NP regions and increased by 26% (9 µm) over polar regions. These changes in the first order retrieval parameters affect the computed values of *WP*, particularly over the polar areas, where the changes are so large. Over NP water and land surfaces, LWP increases by 9% (7 gm^{-2}) and 23% (17 gm^{-2}), respectively. Over polar regions, LWP rose by 242%, on average, in Ed4, with particularly large increases over land. The mean IWP increased by 94%, in the mean.

Comparisons of Ed2 data over continental stratus clouds indicated that τ from Terra and Aqua are biased by -3.6% and 7.8%, respectively, relative to the surface retrievals.(Dong et al. 2008). The corresponding mean values of r_e are biased by only 0.1 and 0.2 µm, while LWP means from Terra and Aqua are 0.6 and 28.1 gm^{-2} greater than the matched surface averages. Thus, it is expected that similar comparisons of Ed4 results with surface observations should yield comparable agreement. Initial comparisons, however, give mixed results.

Xi et al. (2014) compared with Terra and Aqua Ed4 retrievals to observations taken at ARM Mobile Facility at the Azores (Wood et al. 2015) site from June 2009 through December 2010. When averaged over a 30 km x 30 km area, the Ed4 liquid cloud r_e is 1.3 µm greater than the ARM retrievals (12.8 µm), while the Ed4 mean LWP is 13.5gm^{-2} less than its ARM counterpart (114.2 gm^{-2}) due to its smaller optical depth (9.6 versus 13.7). The differences are reduced by 50% when the Edition4A averages are computed using only the MODIS pixel nearest the AMF site. The 10% differences between the ARM and CERES-MODIS LWP and r_e retrievals are within the uncertainties of the ARM LWP (~20 gm^{-2}) and *re* (~10%) retrievals; however, the 30% difference in optical depth is significant. Possible reasons contributing to this discrepancy are increased sensitivities in optical depth from both surface retrievals when τ~10 and topography. The τ differences vary with wind direction and are consistent with the island orography. Much better agreement in τ is obtained when using only those data taken when the wind is from the northeast, where topographical effects on the sampled clouds are minimal.

Those results contrast with those from comparing Terra and Aqua Ed4 retrievals with LWP values measured by a shipborne microwave radiometer (MWR) during the Marine ARM GPCI (Global Energy and Water Cycle Experiment –GEWEX- Cloud System Study –GCSS- Pacific Cross-section Intercomparison) Investigation of Clouds (MAGIC) campaign (Painemal et al. 2015; Zhou et al. 2015). MODIS LWP data from overcast scenes averaged for a area within a 10-km radius of the ship location at each overpass time, were matched with the mean ship LWP for an hour centered on the overpass time. Figure 31 shows a scatter plot of the MAGIC LWP matched with the corresponding Terra and Aqua retrievals. The homogeneous LWP, computed using Eq(6), exceeds the 3-channel MWR LWP by 18.5 gm^{-2} (Figure 31a). Given the mean MWR LWP, 63.8 gm^{-2}, the bias is 29%, in the same direction as the Ed2 comparisons over land (Dong et al. 2008). However, if the adiabatic approximation is applied, the satellite LWP bias is only 4.5 gm^{-2} or 7% (Figure 31b). The standard deviation of the differences is also reduced when using the adiabatic approach. Because of the absence of an island effect, the differences are likely more representative of retrieval acuracy over ocean than the Azores comparisons. These results suggest that the adiabatic approach offers better accuracy, at least , for stratus LWP estimation. This can be easily effected by multiplying the CERES SSF LWP value by 0.833.

Dong et al. (2015) compared overcast stratus properties retrieved with Ed4 code and from surface measurements at the ARM surface site at Barrow, AK for both snow-free and snow-covered conditions. For 90 snow-free cases, they found that the Ed4 r_e is 2.3

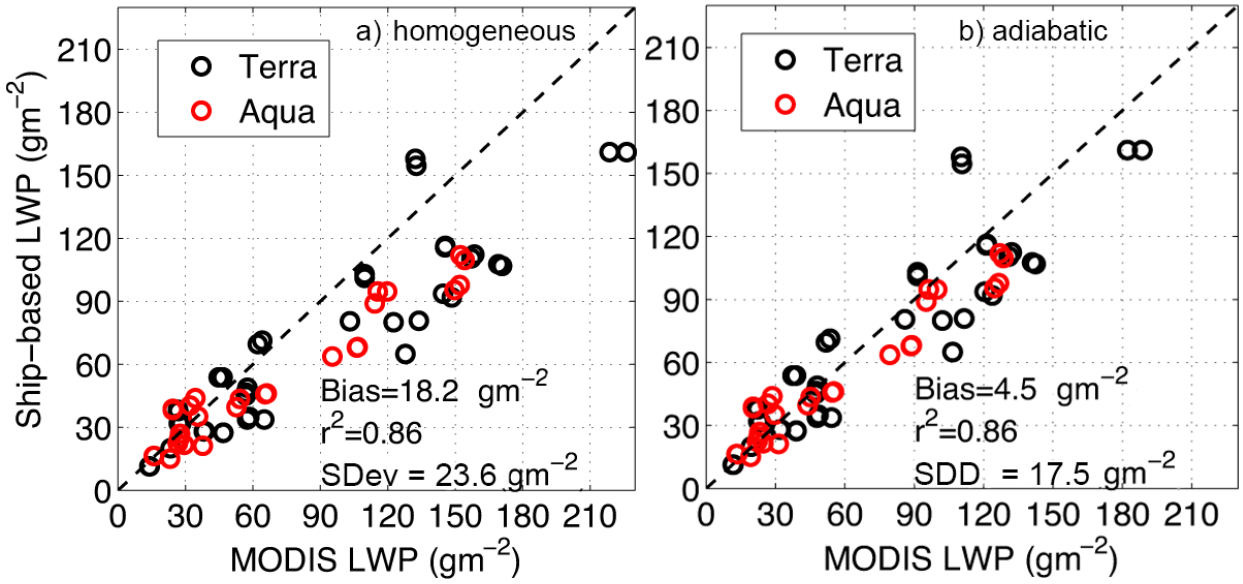

Figure 31. Comparison of Aqua and Terra CERES-MODIS and ARM ship-based cloud LWP values for June-July 2013.

µm (18%) larger, on average, than that found from the surface site. However, the average cloud optical depth is only 0.8 (8%) larger than the surface retrieval. The corresponding mean LWP bias relative to the ARM retrieval is 9.8 gm^{-2} (12%). Using the adiabatic assumption the bias would be –6 gm^{-2} (-7%). For 68 snow-covered cases, the Ed4 r_e and τ biases are 4.5 µm (52%) and -3.2 (-21%), respectively. For these cases, the mean LWP is 21.9 gm^{-2} (24%). Here again, the adiabatic assumption yields an improvement, reducing the bias to 2.9 gm^{-2} (3%). To date, these are the only studies of Ed4 stratus/strtocumulus validation. Assessing the quality of retrievals for other cloud types is difficult because of the broken/scattered nature of the clouds and variations in vertical profiles.

Given the larger values of r_e retrieved using the 2.1-µm channel (Table 9), it can be concluded that LWP computed using those values will be significantly overestimated for most of the stratus cases considered. The one exception is for the Azores matchup, where using the effective radius retrieved using 2.1-µm channel to calculate LWP can reduce the difference between the Ed4 and ARM microwave radiometer retrievals from 13.7 to 2.1 gm^{-2}. Based on the other comparisons, however, it is likely that the bias over the Azores is mainly due to the island effect. Computing LWP using the 1.24-µm channel retrieval is not recommended since the values of r_e from that channel are not usable.

So far, validation of the Ed4 ice cloud properties has been conducted using CALIPSO data and aircraft in situ data. The CALIPSO-based cirrus retrieval method is limited to optically thin clouds and loses reliability for clouds with CALIPSO cloud optical depth, τ_C > 3. It is best for τ_C < 1. Figure 32 compares the SL cirrus retrievals for matched July 2013 CALIPSO and Aqua Ed4 data. During daytime (Figure 32a), the average difference exceeds the mean value of τ_C, with a 200% SDD. The correlation is reasonable, particularly for τ < 2, but a line through the center of the data has a slope of ~2, indicating that the mean Ed4 cirrus optical depth is roughly twice the CALIPSO value during the day. Thus, despite the use of a roughened ice crystal scattering model, the optical depths are similar to those found with Ed2. The asymmetry factors for both the Ed2 and Ed4 are apparently too large to yield the smaller optical depths needed to obtain agreement between the Ed4 and CALIPSO daytime thin cirrus top heights (Figure 26 a-c) and optical depths (Figure 32a). At night, the bulk of the data is centered on the line of agreeement. The bias is 25% with a 100% SDD. When τ_C > 0.5, some of the Ed4 retrievals tend to larger values resulting in the overall bias.

The CALIPSO Version 3 optical depth retrievals use two different methods, constrained (Jossett et al. 2012; Hu et al. 2007) and unconstrained (Young and Vaughan 2009). The latter assumes values for the lidar ratio and layer multiple scattering factor, while the former resolves those values explicitly in the retrieval. While the constrained values are more accurate because they account for the variability in the various parameters, they can only be applied under certain conditions, which are not always met at night and rarely during the day. The comparisons use all data, constrained and unconstrained. Figure 33 shows the optical depth comparisons at night using only constrained retrievals. The results over ocean (Figure 33a) and land (Figure 33b) are nearly identical. The bias and SDD reduced to 5% and 53%, respectively, but the sample volume is only about half of the full dataset (Figure 32b). Similar results were found for daytime cases (not shown), however, the results are not as conclusive since fewer than 100 data points were available for July 2013. The good agreement between τ and τ_C at night is consistent with the relatively small non-opaque cloud-top height biases at night (Figure 26d, e).

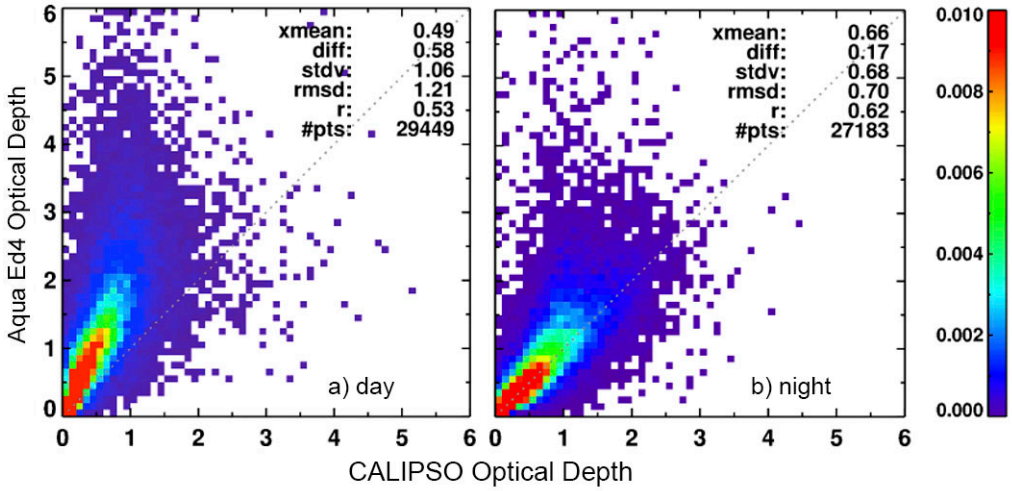

Figure 32. Snowfree July 2013 matched CALIPSO and Aqua Ed4 MODIS optical depths for SL optically thin cirrus clouds, $\tau_C < 3$, over ocean.

Garnier et al. (2015) determined that the error in the unconstrained retrievals depends on cloud temperature and optical depth. To better understand the uncertainties in the Ed4 retrievals, mean biases were computed for 10° intervals of T_e and 0.3 intervals of τ_C. The results are summarized in Figure 34 for day and night unconstrained and night constrained retrievals (left column). The number of samples for each optical depth and temperature range is indicated on the plots in the right half of the figure. The daytime relative errors (Figure 34a) are greatest at the lowest temperatures and relatively constant for $T_e > 215$K for a given optical depth range. The exception is for $\tau_c < 0.3$. In that case, the daytime result appears more like its nighttime counterpart (Figure 34c) with a very small error at 190 K that increases with T_e. This surprising result is most likely due to the use of the 1.38-µm channel to detect very thin cirrus clouds during the day. Once detected, the retrieval mimics the nighttime algorithm, except that the value of T_e is taken from the temperature profile, pressure below 400 hPa where relative humidity is greatest. Clouds having $\tau < 0.3$ are difficult to detect during daytime without the 1.38-µm channel reflectance. With the 1.38-µm channel, however, the number of samples (Figure 34b) are even greater than those for the unconstrained nighttime data (Figure 34d). The daytime sampling for other optical depth ranges maximizes near 235 K, but at lower temperatures for the night cases. Assuming that the distributions should be similar day and night, this difference reflects the overestimate of τ, which results in greater values of T_e.

The nighttime unconstrained and constrained (Figure 34e) biases are similar for colder clouds but diverge for warmer clouds, which generally have smaller errors for the constrained matches. Additionally, very few clouds with $\tau_c < 0.3$ remain in the constrained sample set. A constrained retrieval is rarely attempted for $\tau_c < 0.3$ because of the large uncertainties (Garner et al. 2015). There is a slight underestimate for $\tau_c > 0.3$ for both sets when $T_e < 225$ K. The constrained dataset eliminates many of the cases having large uncertainties, which reduces the differences between relative errors and sampling for the various τ_c intervals. Validation of optical depth for thicker ice clouds is more difficult because of great variations in cloud particle habits, size, phase, and water content

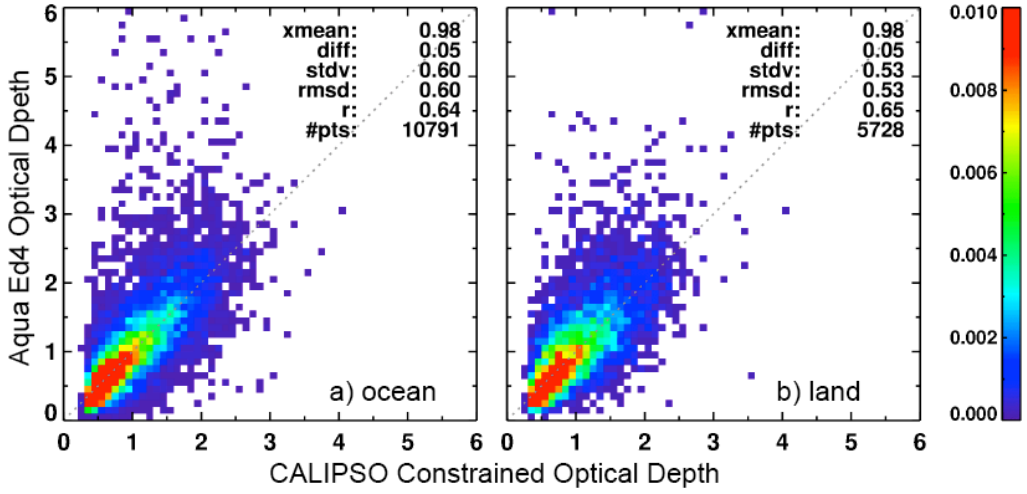

Figure 33. Snowfree July 2013 matched CALIPSO constrained and Aqua Ed4 MODIS optical depths for SL optically thin cirrus clouds, $\tau_C < 3$, at night.

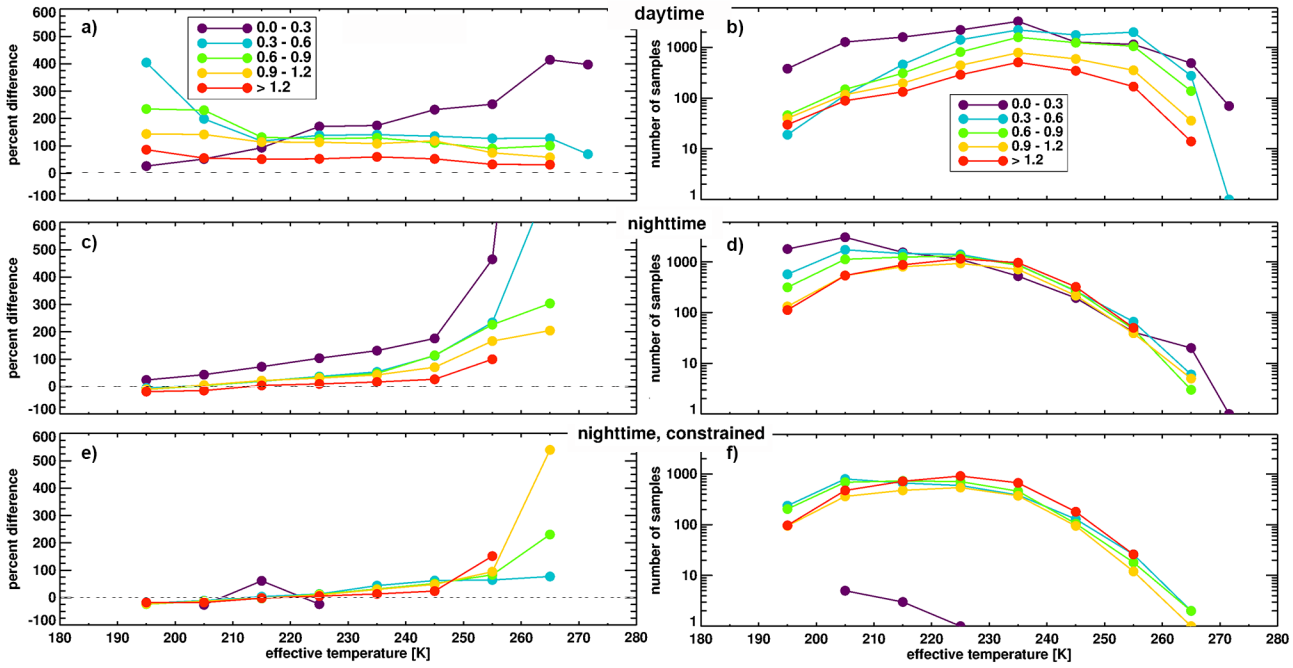

Figure 34. Snowfree July 2013 matched CALIPSO constrained and Aqua Ed4 MODIS optical depths for SL optically thin cirrus clouds, $\tau_C < 3$, at night.

under the upper layer cloud. Generally, it is more straightforward to compare IWP values and infer from them the accuracy of the optical depths. IWP comparisons are discussed below.

Ice cloud particle size and habit tend to vary with altitude or temperature, while the value of r_e retrieved using the 3.8-µm channel generally corresponds to the upper 1-3 optical depths of the cloud (Chang and Li, 2002). Thus, for thin ice clouds, the value of r_e(3.8) should generally be representative of the entire cloud. Mace et al. (2005) found that r_e(3.8) from CERES Ed2 underestimated the radar retrieval in cirrus with $\tau < 2.2$ by 2.9 µm. Given the average increase of 1.9 µm in r_e relative to Ed2 for non-polar land (Table 7), it is expected that the Ed4 r_e value would be closer than its Ed2 predecessor for those cases. For thick ice clouds, it is expected that

the value of r_e(3.8) will be less than that for the entire cloud because the sizes tend to increase with temperature. A preliminary comparison of r_e from MODIS with in situ measurements taken during the Studies of Emissions and Atmospheric Composition, Clouds and Climate Coupling by Regional Surveys *(SEAC4RS)* field program characterizes the relationship between the retrieved and in situ values of r_e. Figure 35 shows the average r_e within from the 2D-S probe on the DC-8 aircraft for all flights during the experiment for times within 30 minutes of the Terra or Aqua overpass. The means were computed for layers corresponding to the normalized depth of the aircraft from cloud top as determined by the satellite. Because of uncertainties in the retrieved cloud-top

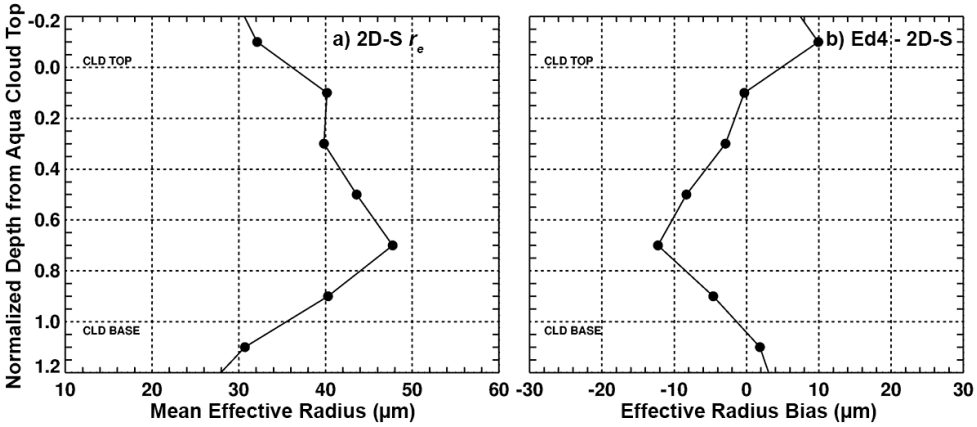

Figure 35. Mean ice crystal (a) effective radius from DC-8 2D-S probe and (b) mean effective radius difference between CERES Ed4 and 2D-S for matched flight segments and Aqua MODIS pixels as a function of the normalized depth below the cloud-top height from the Ed4 Aqua retrieval.

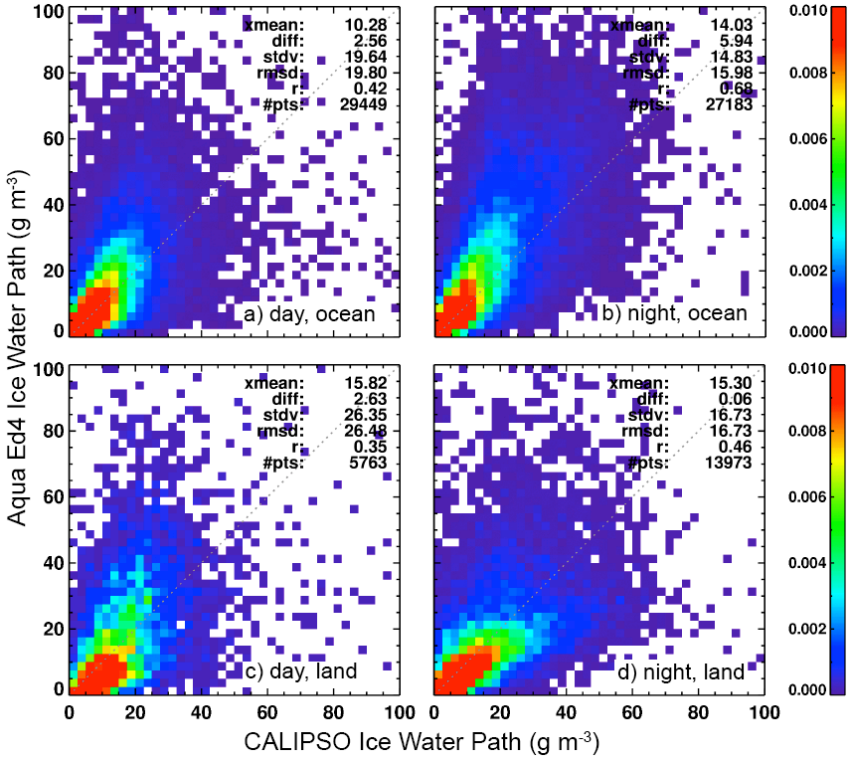

Figure 36. Snowfree July 2013 matched CALIPSO and Aqua Ed4 MODIS IWP for SL optically thin cirrus clouds, $\tau_C < 3$.

and base heights, some of the layers appear to be outside of the cloud boundaries. Thus, instead of five 0.2-intervals, seven are used. The profile of r_e(2D-S) shows that it is smaller at the top and increases to a point corresponding to a depth of 0.7 in the cloud before decreasing to cloud base (Figure 35a). Figure 35b shows that the mean differences between the MODIS Ed4 retrieval and the

2D-S probe are positive above the 0.1 level and become negative as low as -10 µm at 0.7 before increasing again. This behavior is expected. The absolute values of the differences may be not particularly accurate as these are preliminary data and the 2D-S probe does not measure particle radius smaller than 5 µm and likely underestimates concentrations for sizes smaller than 10 µm (Lawson et al. 2006). The vertical changes, however, are likely to be representative of the relative vertical profiles.

CALIPSO ice water path retrievals (Garnier et al. 2013) are compared to those from Aqua Ed4 in Figure 36. The bulk of the data lie on the 1:1 line for clouds over ocean during both day (Figure 36a) and night (Figure 36b) for $IWP_c < 20$ gm^{-2}. At greater IWPc values, the Ed4 retrievals are larger. The day and night biases are 25 and 42%, respectively, with SDDs of 191 and 100%. Over land, the data for $IWP_c < 20$ gm^{-2} tend to be underestimated and are overestimated for larger IWP_c values. The resulting day (Figure 36c) and night (Figure 36d) biases are 17 and 0%, respectively, with SDDs of 167 and 111%. Apparently, the retrieved values of re during the day offset the overestimate of τ, resulting in smaller errors in IWP. Waliser et al. (2009) found very good correspondence between average IWP distributions from CloudSat and Ed2 retrievals. Similar results are expected for Ed4 since the mean IWP for nonpolar areas is nearly identical to that of Ed2 (Table 7). Over polar regions, Ed4 IWP is about double the Ed2 value, but in Waliser et al. (2009), Ed2 underestimates IWP in polar regions. The Ed2 and Ed4 IWP and LWP values are actually estimates of the total column water path (TWP) since it is assumed that the cloud is single phase and single-layered. If liquid water is in the column below the ice cloud, its contributions to the reflectance will be interpreted as if it were ice. Smith (2014) compared TWP derived for thick ice-topped clouds from radar and radiometer data with Ed4 IWP values over the ARM SGP site. He found excellent agreement between the surface-based TWP and a surrogate Ed4 IWP from GOES data for IWP < 500 gm^{-2}. For larger values, IWP underestimated TWP by 15% for TWP = 1000 gm^{-2} up to 25% for TWP = 4000 gm^{-2}. Thus, for IWP > 500 gm^{-2}, it is expected that the true IWP is greater than the retrieved value.

The viewing angle dependence of daytime optical depth, particle effective radius, and water path are plotted in Figure 37, Figure 38, and Figure 39, respectively. Over ocean, liquid cloud τ decreases by 9% between 5° and 65° (Figure 37a), while over land it drops by 18%, possibly due to more convective clouds over land. The ocean ice cloud τ decreases by 17% compared to 30% over land (Figure 37b). Conversely, the retrieved r_e values tend to increase with VZA (Figure 38). Over ocean, droplet effective radius increases by only 5%, while over land it rises by 7% (Figure 38a). Ice cloud particles show greater changes with re increasing by 8 and 13% over ocean and land, respectively (Figure 38b).

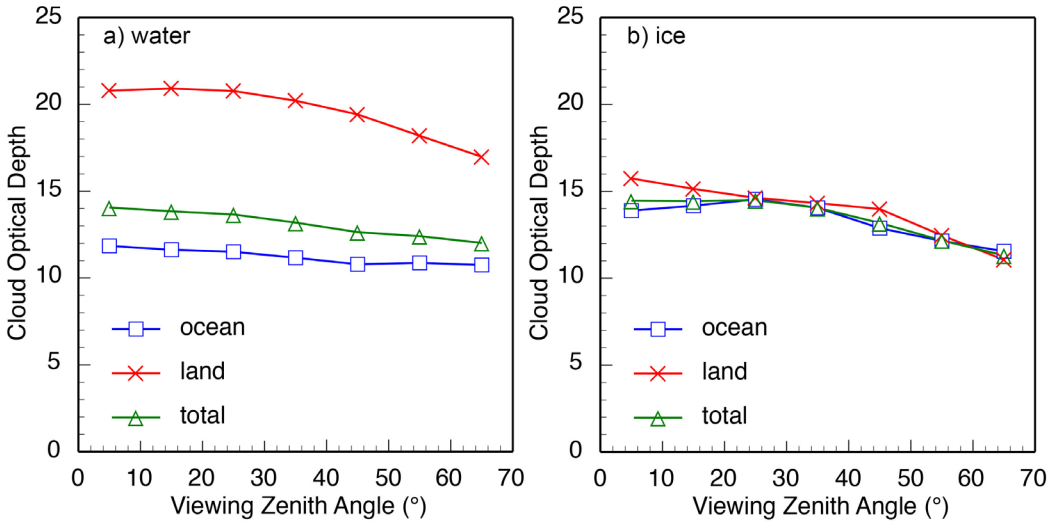

Figure 37. Mean 2004 global cloud optical depth from Aqua CERES-MODIS as a function of viewing zenith angle.

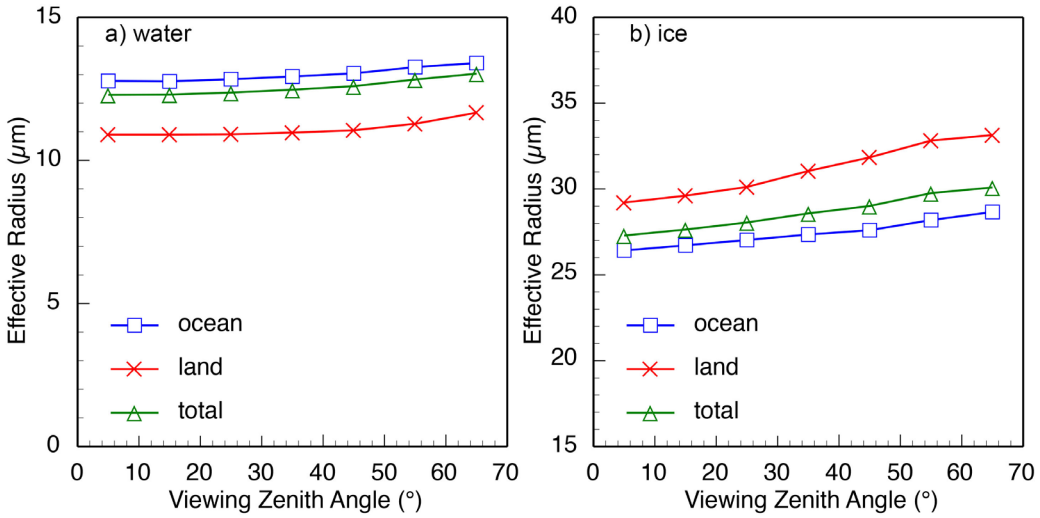

Figure 38. Mean 2004 global cloud particle effectiveradius from Aqua CERES-MODIS as a function of viewing zenith angle.

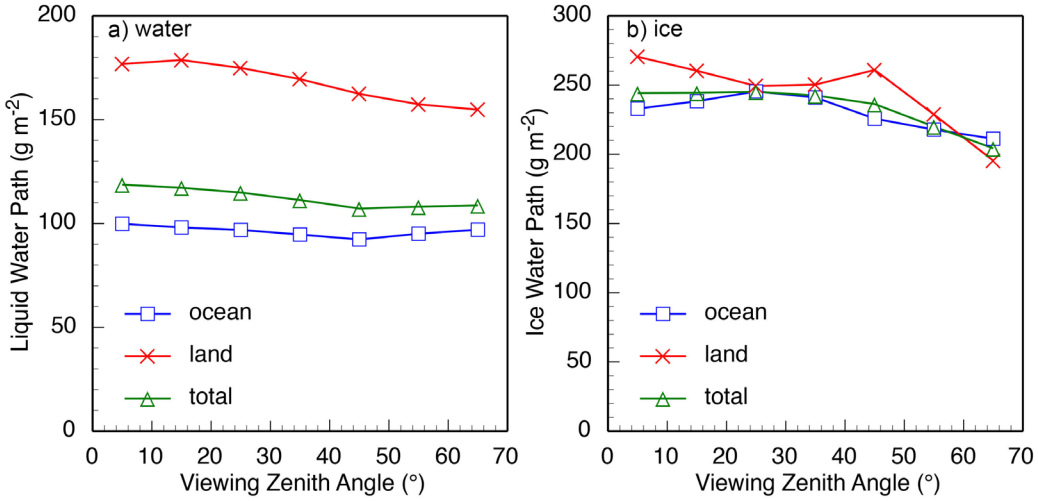

Figure 39. Mean 2004 global cloud water path from Aqua CERES-MODIS as a function of viewing zenith angle.

The changes partially complement each either such that the LWP is nearly flat over ocean and drops by only 13% over land (Figure 39a). Mean IWP decreases by 9% over ocean and 28% over land (Figure 39b). These changes are likely due to vertical structure in the clouds that is not accounted for in the plane parallel model used in the retrievals.

Validation of the CERES products is an ongoing effort. The results presented here are intial assessements of the results. Future studies will attempt to shed more light on the quality of the Ed4 data cloud products.

Return to Quality Summary for: SSF Terra-Aqua Edition4A.